THE ASTRONOMICAL JOURNAL VOLUME 107, NUMBER 1 JANUARY 1994

MEAN MORPHOLOGICAL TYPES OF BRIGHT GALAXIES

R. BUTA
Department of Physics and Astronomy, University of Alabama, Tuscaloosa, Alabama 35487
Electronic mail: buta@ualvm.bitnet

S. MITRA AND G. DE VAUCOULEURS
Department of Astronomy, University of Texas, Austin, Texas 78712
Electronic mail: gav@astro.as.utexas.edu

H. G. CORWIN, JR.
IPAC, M/S 100-22, Caltech, Pasadena, California 91125
Electronic mail: hgcjr@ipac.caltech.edu

Received 1993 June 21; revised 1993 September 7

ABSTRACT

The revised Hubble classifications provided in the *Third Reference Catalogue of Bright Galaxies* are based on nine lists and catalogues, both published and unpublished, from five observers. This paper describes the procedures that were used to combine these classifications into mean classifications including the family, variety, and stage. The best classifications in RC3 are based on large-scale photographic images taken with 1.5–5 m class reflectors. However, most of the types in RC3 are based on the small-scale prints, plates, and films of the first Palomar Sky Survey and the UK Schmidt IIIa-J Southern Sky Survey. The overlap between the different observers' samples allowed determination of the reliability of sky survey types and the effects of diameter and inclination on the accuracy of these types. We find that for a typical galaxy having isophotal diameter $D_{25} \approx 2'$ and inclined by $\approx 50°$, types T from the sky surveys have a mean error (averaged over all of the observers) of $\sigma(T) = 0.7$ step on the numerical scale of the revised Hubble system. With the new database of classifications, we rederive the classical relations between Hubble type and integrated colors, surface brightnesses, and hydrogen index (hydrogen flux to blue light ratio) for a large sample of galaxies. We also present a table of galaxies which we consider to be representative examples of each type.

1. INTRODUCTION

One phase in the preparation of the *Third Reference Catalogue of Bright Galaxies* (RC3, de Vaucouleurs *et al.* 1991) was to compile a homogeneous list of *mean morphological Hubble types* of galaxies, based on the several available sources of such types that have been published before and since the publication of the *Second Reference Catalogue of Bright Galaxies* (RC2, de Vaucouleurs *et al.* 1976). These types are an important part of RC3, not only because of the well known capabilities of the revised Hubble system in discriminating galaxy properties (de Vaucouleurs 1977), but also because types are often a necessary starting point in the study of galaxies (de Vaucouleurs 1963). However, morphological types are subjective (being based on visual inspections of photographic images) and as such it is important to examine how reproducible are the types estimated by different observers in a given classification system. The revised Hubble type estimated by a trained observer is analogous to the HD or MK spectral types for stars, which are also visually estimated and whose usefulness in stellar studies has been amply demonstrated. As Otto Struve remarked many years ago, "Without the Henry Draper Catalogue, astronomy of the 20th century would have been a very different science."

To produce the mean types in RC3, we combined type estimates from nine different sources after performing detailed comparisons and reduction to a uniform system with appropriate weights. The present report describes the analysis and procedures used. We also reexamine the dependence on type of various parameters (integrated colors, mean surface brightness, hydrogen index) as was done by de Vaucouleurs (1977) for the RC2, and we provide a small list of galaxies which are representative of a given type.

2. CLASSIFICATION SYSTEM

The types in RC3 use the precepts and notation of the *revised* Hubble system of de Vaucouleurs (1956, 1959, 1963). This system is a refinement of the original Hubble (1926) system that provides more information about the morphology of a galaxy without being too unwieldy. The classification system is defined for images recorded on "ordinary" (i.e., blue-sensitive) emulsions. There are four recognized *classes*: ellipticals E, lenticulars L (or S0), spirals S, and irregulars I. The spiral *families* are denoted by SA for ordinary (nonbarred) spirals, SB for barred spirals, and SAB for intermediate (or weakly) barred cases. Similar notation is used for lenticulars: LA0, LAB0, and LB0. In both the spiral and lenticular families two main *varieties* are recognized. Galaxies which have an inner ring are de-

 0004-6256/94/107(1)/118/17/$0.90

noted by (r) and those whose arms start from the nucleus or the ends of a bar are denoted by (s). Intermediate varieties are represented by (rs). Four main *stages* are distinguished along each of the spiral sequences SA(r), SA(s), SB(r), and SB(s) and are denoted as a, b, c, and d. The intermediate stages are ab, bc, and cd. Spiral stages later than d and similar to the Magellanic Clouds are represented by m, with a transition stage between d and m labeled as dm. Finally, the armless Magellanic irregulars are classified as IAm, IBm, or just Im.

The signs "+" and "−" are used to denote late and early types, respectively. In both the SA0 and SB0 subclasses the three stages are described as L^-, L^0, and L^+.[1] The ellipticals are classified as compact ellipticals (cE) and normal ellipticals (E), with a class E^+ used initially in the *Reference Catalogue of Bright Galaxies* (de Vaucouleurs & de Vaucouleurs 1964, hereafter RC1) for a possible transition stage to S0, and later in RC2 for the supergiant cD systems. Those galaxies which have an external ring are represented by (R) preceding the classification of the basic type. When the outer arms are so tightly wound that they mimic an external ring, the notation (R′) is used to denote the presence of a pseudoring.

The family, variety, and stage are thus three parameters which describe spiral and lenticular galaxies. The complete classification system is three-dimensional and can be looked upon as a grid of 121 cells, but in reality there is a continuous variation in the three parameters and galaxies can occupy any point in the classification volume [Fig. 1 (Plate 22)].

3. MEAN REVISED HUBBLE TYPES

Prior to RC3, there was little attempt to combine classifications by different, independent observers into some kind of mean type. Firstly, the various classification systems usually had only one major proponent, and were sufficiently different and personal that combining types was not practical (de Vaucouleurs 1963). Secondly, different observers applying a system would use different image material (e.g., large-scale plates versus sky survey images), and it is not prudent to combine such types without knowing how reliable they are. Finally, it is not entirely clear how to combine morphological types, which are not objectively measured quantities.

For RC3, types in the revised Hubble system were available from nine sources. The only practical way of combining these types was to assign a numerical index to the various parts of a classification. The stage index T, introduced in RC1 and also used in RC2 and RC3, is an arbitrary numerical index that has proven convenient for many applications. It was used in our analysis and is summarized in Table 1. Indices were also assigned to family and variety characteristics and are discussed in Sec. 4.

[1]Because of the poor correlation between the L^-, L^0, and L^+ types and the $S0_1$, $S0_2$, and $S0_3$ types in the Hubble Atlas (de Vaucouleurs 1963), they could be used in combination to provide the basis of an improved classification.

TABLE 1. Coding of revised Hubble stage.

Stage	T	Stage	T
cE	−6	Sb	3
E	−5	Sbc	4
E^+	−4	Sc	5
$S0^-$	−3	Scd	6
$S0^0$	−2	Sd	7
$S0^+$	−1	Sdm	8
S0/a	0	Sm	9
Sa	1	Im	10
Sab	2	cI	11

Previous work has indicated that the revised Hubble system is reproducible by independent observers (Corwin 1970; Buta 1978). The present study reconfirms this point. It is, therefore, possible to combine most of the galaxy types in this system that are available in the literature, and to calculate weighted mean numerical types with well defined mean errors. Our intention was not only to produce a catalogue of mean types of galaxies, but also a subset of galaxies useable as standards that are representative of their types, i.e., with low mean error or with two or more observations.

3.1 Selection of Source Catalogues

The galaxy types used in our study were taken from the sources listed in Table 2. A numerical value was assigned to each stage of the types according to Table 1. The UGC types were placed on the RC2 system by Corwin. The types from the ESO catalogue (Lauberts 1982) were not included since they are not strictly on the revised Hubble system and were only intended as rough estimates. The types given in the *Revised Shapley-Ames Catalogue of Bright Galaxies* (Sandage & Tammann 1987) were also not used since there are significant departures from the RC2 system and objective tests show that the latter agrees better with quantitative parameters (de Vaucouleurs & Corwin 1986).[2]

The production of the catalogue of mean Hubble types was a two-phase project because the last four sources in Table 2 (ESGC, CSRG, Skiff, and Hercules) were not available when the original analysis was carried out. For this reason we divide our discussion into two parts. Firstly, we describe the production of the *Mean Type Catalogue*, or MTC, prepared mainly by Mitra using only the first five sources in Table 2 and involving only the mean numerical stage index T. Secondly, we describe the addition of the four later sources and the computation, mainly by Buta, of the mean *full* types (i.e., taking into account family and variety) used to produce the *Revised Mean Type Catalogue*, or RMTC, incorporated in RC3.

[2]This is particularly true for types later than Sc which are underrepresented in RSA where many are misclassified as Sc. However, we believe that for early-type spirals (Sa, Sab) the RSA types are often preferable to the RC2 types listed as S0 or S0/a, when the latter are based on small-scale survey plates. Unfortunately, we could not quantify this distinction to make it amenable to statistical treatment.

TABLE 2. Source catalogues.

RC3 Code	Number of Galaxies	Acronym	Reference	Image Material
R	1993	RC2	de Vaucouleurs et al. (1976)	large-scale reflector plates
P	1104	RC2 PSS	Corwin (1968,1970)	PSS I prints or copy plates
C	112	-	Corwin (1968,1970) not in RC2	PSS I prints or copy plates
B	226	-	Buta (1978)	PSS I prints (Whiteoak Ext.)
U	8610	UGC, UGCA	Nilson (1973, 1974)	PSS I prints
S	4711	SGC	Corwin et al. (1985)	UK IIIa-J plates, copy plates, films
E	2524	ESGC	Corwin and Skiff, in prep.	PSS I copy plates
F	721	-	Skiff, in prep.	UK Schmidt asteroid survey plates
r	1351	CSRG I	Buta, in prep.	UK IIIa-J and ESO-B copy films
H	145	Hercules Cl.	Buta and Corwin (1986)	KPNO 4-m copy films

3.2 Phase 1: The Mean Type Catalogue

The *Mean Type Catalogue* was computed by assigning a quantitative weight to each of the first five sources in Table 2. This external weight depends not only on the consistency and experience of the classifier, but also on the size of the galaxy and its inclination (these latter characteristics are obtained from the isophotal parameters log D_{25} and log R_{25}, respectively). Moreover, all of these sources had a qualitative or quantitative internal estimate of the uncertainty of the classification. We used the weight assigned by the classifier as the internal weight. The product of the external and internal weights gives the combined weight. For a single observation, this combined weight is a measure of the mean error of each classification. For multiply-observed objects, the combined weights can be used to calculate a weighted mean type and a mean error.

The initial step was to assign an external weight to each of the sources for unit internal weight. For our reference system, we chose the system as defined by the RC2. The stage index T, its uncertainty symbol and weight, and the type source were extracted for all available objects with the following exceptions: (1) all types from the source "P048" because these were galaxies classified from PSS prints; (2) all I0 galaxies having type "0" and those peculiar galaxies that had "R" (ring galaxy) or "P" (peculiar) attached to their type.

The catalogue of Buta (1978) was based on inspection of the Whiteoak Extension of the Palomar Sky Survey. It includes revised Hubble classifications for 412 NGC and IC galaxies only. The classifications were assigned relative weights on a scale from 1.0 to 3.0 to at least qualitatively allow for the added uncertainties due to overexposure, small image size, and the graininess of the print copies. For galaxies in common with RC2, we entered the types, uncertainty symbols, and weights from this catalogue into our database. The two lists by Corwin (1968, 1970) are also based on print copies of the PSS, and for these we also included uncertainty symbols in our analysis. Many of Corwin's types from these lists were used in RC2 and are indicated as source P in RC3. We will take sources C and P to be the same. Since none of these catalogues had diameter or axis ratio information, these parameters were taken from RC2.

The diameters and axis ratios from the UGC were reduced to the standard RC2 systems using transformation relations and coefficients given in the introduction to RC2. We assumed that the same coefficients applied to the UGC Supplement as well. It was necessary, however, to derive transformation relations for the SGC diameters and axis ratios since these were not available at the time we started our analysis [see Paturel *et al.* (1991) for the final relations adopted in RC3]. A list of galaxies common to the RC2 and SGC was drawn, and the diameters and axis ratios compared. Those galaxies having m.e.(log D_{25}) $\geqslant$ 0.14 and m.e.(log R_{25}) $\geqslant$ 0.14 in the RC2 system were rejected. Since the SGC gives weights for diameters and axis ratios, those SGC galaxies having $w(\log D) < 0.5$ and $w(\log R) < 0.5$ were rejected. Impartial linear least-squares fits were made between the two estimates of log D and log R and the coefficients were determined after one cycle of 2σ rejections:

$$\log D_{25} = (1.000 \pm 0.002) \log D - 0.276, \quad (1a)$$

$$\log R_{25} = (1.214 \pm 0.029) \log R - 0.008. \quad (1b)$$

These relations were used to reduce all the SGC diameters and axis ratios to the RC2 system. For the galaxies in common to RC2 and SGC, weighted mean diameters and axis ratios were calculated. Using the codes "R" and "S" to represent the RC2 and SGC, respectively (Table 2), the weighted mean was given by

$$\langle \log D_{25} \rangle = W_R \log D_R + W_S \log D_S, \quad (2a)$$

$$\langle \log R_{25} \rangle = W_R \log R_R + W_S \log R_S. \quad (2b)$$

If e_R is the mean error as given in the RC2 and w_S the weight as given in SGC, then the weights W_R and W_S were determined as follows:

if $(e_R > 0.1)$ and $(w_S > 0.25)$

then $W_R = 0.33$ and $W_S = 0.67$,

if $(e_R > 0.1)$ and $(w_S \leqslant 0.25)$

then $W_R = 0.50$ and $W_S = 0.50$,

if $(e_R \leqslant 0.1)$ and $(w_S > 0.25)$

then $W_R = 0.50$ and $W_S = 0.50$,

if $(e_R \leqslant 0.1)$ and $(w_S \leqslant 0.25)$

then $W_R = 0.67$ and $W_S = 0.33$.

For the estimation of external type weights $W_e = (\text{m.e.})_e^{-2}$, we chose from our combined listing those galaxies that had no uncertainty symbols. These were the

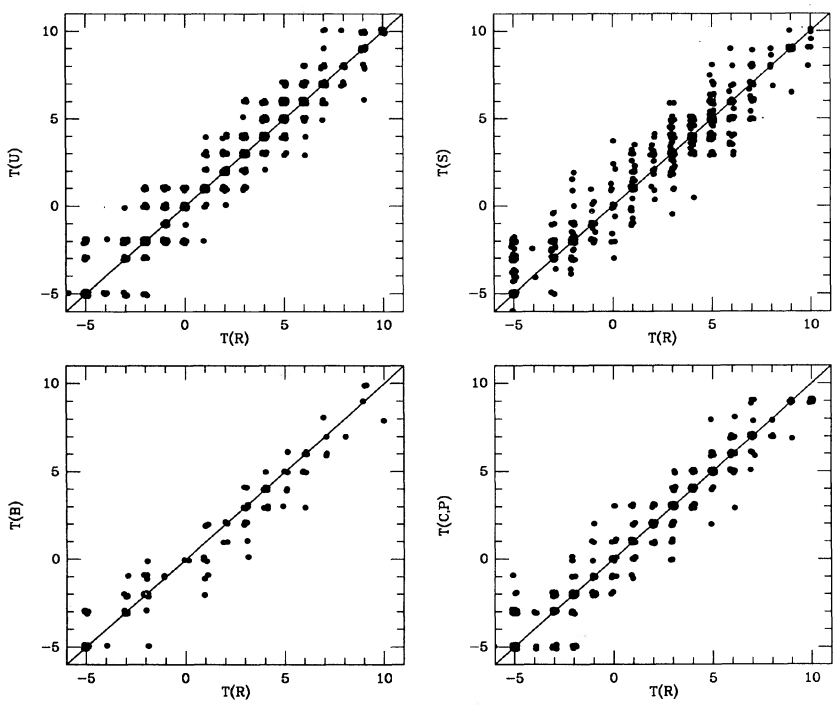

FIG. 2. Comparison between type estimates from small-scale sky survey sources U, S, B, and C, P with the large-scale reflector plate types from RC2. A random number generator has been used to slightly offset overlapping points since input types have integer values.

galaxies that were best classified according to the classifier. Since the SGC galaxies had no uncertainty symbols, the galaxies with weights 1.00 or greater were chosen. We then made a comparison of the types taking the catalogues two by two. With five sources there were 10 possible combinations, but only nine could be used because there are no galaxies in common between Buta's catalogue and the UGC. For each comparison, we computed the variance

$$\sigma_{ij}^2=\frac{\Sigma(T_i-T_j)^2}{N_{ij}} \tag{3}$$

for catalogues i and j. Under the assumption that the sources are independent, we can write

$$\sigma_{ij}^2=\sigma_i^2+\sigma_j^2. \tag{4}$$

The nine possible combinations give us nine equations in five unknowns: the individual errors for the five sources, which we denote σ_R for RC2, σ_B for Buta (1978), σ_C for Corwin (1968, 1970), σ_S for SGC, and σ_U for UGC. The least-squares method of obtaining these errors for the respective catalogues is described by de Vaucouleurs & Head (1978). The solutions gave the error associated with each catalogue: $\sigma_R=0.30$, $\sigma_B=0.45$, $\sigma_{C,P}=0.65$, $\sigma_S=1.00$, and $\sigma_U=0.50$, for types of unit internal weight. Figure 2 illustrates the comparisons between the standard RC2 types and the four PSS sources. Whenever a type had an uncertainty symbol, this was used as an estimate of its internal weight. Values of 0.5 were assigned to the symbol ":" and 0.25 to the symbol "?". Otherwise unit internal weight was assigned. In the case of the SGC, the listed numerical weight was used as the internal weight.

To evaluate the effect of the size of a galaxy on the error in its classification, which primarily depends on the number of resolution elements in the image (see de Vaucouleurs 1963 and RC2, p. 15), we made a least-squares solution of the following equation:

$$\Delta T=|T_i-T_j|$$
$$=a+b(2\log D-\log R-\langle 2\log D-\log R\rangle), \tag{5}$$

where $\langle 2\log D-\log R\rangle=2.89$. Those galaxies that had $\Delta T\geqslant 5$ were rejected from the solution, which gave the values $a=0.567\pm0.020$ and $b=-0.189\pm0.034$, respectively. Remembering that for a Gaussian distribution, the mean error $\approx 1.25\times$ the average deviation, the following expression was adopted for the external mean error:

$$(\text{m.e.})_e=\sigma[1-0.2(2\log D-\log R-2.89)/\sigma]. \tag{6}$$

Here σ is the mean error for each catalogue as given above.

Having estimates of both internal and external mean error and weight, the total weight is given by

$$W=W_eW_i \tag{7}$$

and the mean type and mean error by

$$\langle T\rangle=\Sigma(WT)/\Sigma W, \tag{8a}$$

$$\text{m.e.}(\langle T\rangle)=1/\sqrt{\Sigma W}. \tag{8b}$$

According to this formulation, a very large galaxy would have an unrealistically small mean error in its type. It was decided that the smallest acceptable mean error was 0.3,

which was automatically assigned whenever the calculated mean error was less than 0.3.

The final MTC was compiled by adding all of the galaxies that were not part of the error analysis. These include galaxies from RC2 that were from the Palomar 48 in. prints or plates (sources P048 or P048G) and the remaining galaxies from the SGC and UGC. For the galaxies in common to RC2 and SGC, weighted mean diameters and axis ratios were used. If the difference between any two types for a given galaxy was $\geqslant 4$ all the entries were carefully examined, and a judgment was made as to which entry may be discrepant. The offending type was then removed and the mean type and mean error recalculated.

3.3 Phase 2: The Revised Mean Type Catalogue

The MTC as described above was based on the five major catalogues of revised Hubble types available prior to 1985. In 1988, three additional and substantial sources of types became available: (1) the Extension to the Southern Galaxy Catalogue (ESGC) by H. Corwin and B. Skiff (unpublished), which covers the poorly studied zone in the declination range $-2°$ to $-17°$ based on glass copies of the Palomar I Sky Survey; (2) types based on asteroid survey plate fields near the ecliptic by B. Skiff from United Kingdom (UK) Schmidt IIIa-J plates; and (3) phase I of the *Catalogue of Southern Ringed Galaxies* (CSRG) by R. Buta (see Buta 1991), which includes mainly galaxies with inner and outer rings and pseudorings as identified on the SRC-J southern sky survey. These sources provided 3673, 1304, and 1975 type estimates, respectively. Also, Buta & Corwin (1986) published an extensive list of types for over 200 galaxies in the Hercules Supercluster region, based in part on high quality film copies of six KPNO 4 m telescope prime focus plates. All of these sources provided useful additional information for RC3, and we decided to incorporate them into the final catalogue.

The compilation of the *Revised Mean Type Catalogue*, or RMTC, was carried out as follows. Since it was clearly impractical to repeat the MTC analysis completely to incorporate these new sources, the approach we used was to compare each of the new sources with the mean types already in the MTC, and then we derived the relevant least-squares relations and external mean errors from those comparisons alone. Once these quantities were known, the new sources were incorporated into the MTC. At the same time, it was necessary to compute for each galaxy a mean *full type*, that is, the coded type specifying the family, variety, outer ring, etc. These types were not a part of the MTC.

3.4 Parameters of the New Sources

The type data for each of the new sources were available in separate files as raw full types, e.g., SAB(rs)bc. For each file, we computed a rewritten version which used, where available, catalogue names for non-NGC/IC galaxies instead of pure anonymous (or positional) names. The alternate names were UGC, UGCA, MCG, and ESO, and serve to identify an object when positional names are ambiguous. At the same time, the raw types, were read character by character to get a computer-estimated "T" value following the RC2 convention (Table 1).

A series of programs was written to identify all galaxies in the four new lists of types in common with the MTC, and to make lists of those not found. Those in common were output in a file which identified the index the object has in the MTC, to facilitate adding the new T values to those already available as well as comparing these with the mean types in the MTC. In the cases of the ESGC and the Skiff samples, we also took into account whether a type was uncertain (:) or doubtful (?). In the case of the CSRG, very few of the objects had such symbols because the ringed galaxy sample selected those galaxies where bars and rings were detectable and measureable and does not include too many where such features were only a suspicion or not well resolved. The sample therefore selected mainly the galaxies best defined for morphology. In the Hercules sample, a comparison with the MTC was not useful as very few were found in common and most Hercules types in the various catalogues were based on the PSS prints. For Hercules, we refer instead to the results from a comparison with types obtained by Dressler (1980) based on Las Campanas 2.5 m plates, which are better than PSS types and more suited to comparisons with 4 m types (see Buta & Corwin 1986).

Several problems were encountered in the comparisons with the MTC. The most serious concerns objects whose name in one of the new lists is not consistent with the name in the MTC. Any object not found in MTC by name was always checked by position using a tolerance of 1'.75 to allow for roundoff error. This inevitably means that in some cases either the wrong object will be found or two objects will be found implying that a galaxy is part of a pair. We wrote programs to try and sift out these mismatches. This problem underlines the need for *consistency* in name usage and accuracy in positions.

3.5 Revised Mean T values

Comparisons between sources ESGC, CSRG, and Skiff and the types in the MTC are illustrated in Fig. 3. Initially, we made plots like these and identified all of the discrepant cases. In some cases discrepancies were only identity mismatches with the MTC, but others were genuine observer disagreements. The numbers of objects in common between the MTC and the other lists were 1406 for ESGC, 203 for Skiff, and 920 for CSRG. In addition, for ESGC there were adequate samples of objects in the : and ? categories so that separate least squares solutions could be made for them. For the others these samples were inadequate, but a solution was done for Skiff's : and ? types. Note that Fig. 3 illustrates the comparisons for the more certain types only (no : or ?).

The results showed first that slopes of the impartial line[3] between the new sources and the MTC are less than unity

[3]The bisector of the two regression lines $y(x)$ and $x(y)$, assuming equal precision in x and y; for a recent reference, see Feigelson & Babu (1992).

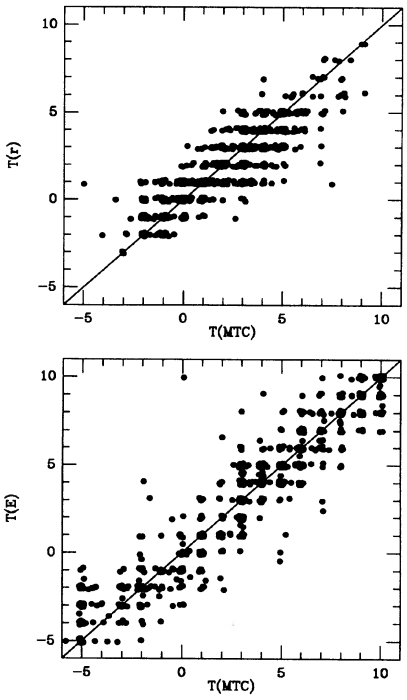

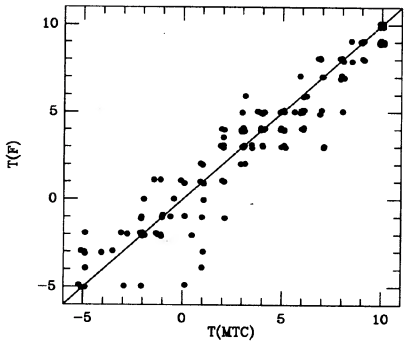

FIG. 3. Comparison between type estimates from sources E, F, and r with the Mean Type Catalogue (MTC). As in Fig. 2, a random number generator has been applied to offset overlapping points.

for all of the three main sources, though for ESGC and Skiff it is not significantly different from unity. Secondly, mean differences $\langle T-T(\mathrm{MTC})\rangle$ were found to be fairly small in each case. However, for the Buta CSRG types, a small but significant scale difference (in the sense of a compression) was found compared to MTC types. Part of the problem here is that the CSRG covers a somewhat narrower range of types than the others since rings are mostly found between types $S0^+$ and Scd. Nevertheless, we adopted in RC3 the following mean relation to reduce the CSRG types to the system of the MTC:

$$T_r^c=2.36+(1.15\pm0.02)[T_r-2.15], \quad (9)$$

based on 920 objects, while for the other sources no scale correction was made.

After correction for scale error, if any, we then computed the dispersion, σ_{xy}, of the difference, $T-T(\mathrm{MTC})$ [or $T^c-T(\mathrm{MTC})$ for the CSRG], where x refers to the MTC and y refers to the new sources. The MTC gives final mean errors for the mean types, and we calculated the mean error σ_y as

$$\sigma_y=\sqrt{(\sigma_{xy}^2-\langle\sigma_x\rangle^2)}. \quad (10)$$

where $\langle\sigma_x\rangle$ is the average mean error over all the galaxies used for the comparison, taken from the MTC. However, to compare these values with those obtained for the initial five sources, we had to reduce them to constant galaxy area, via $\log D_{25}$ and $\log R_{25}$. These dimensions were contained in the MTC, and we computed the reduced mean error σ_{0y} using Eq. (5) above in the form

$$\sigma_{0y}=\sigma_y+0.2(2\langle\log D_{25}\rangle-\langle\log R_{25}\rangle-2.89), \quad (11)$$

where the mean dimensions are averages over all galaxies used in the solution. For the best types (i.e., not : or ?), the mean errors for the new sources are $\sigma_E=0.92$, $\sigma_F=0.87$, and $\sigma_r=0.74$, using the codes in Table 2 (from RC3).

The mean errors for the sky survey sources range from 0.45 to 1.00 type step, with the smallest errors being obtained for sources B, C, and U, even though types from sources S, E, F, and r are based on better image material. We decided that the lack of adequate overlap between all of the sources means that we can use these errors only as an indication of the reliability of sky survey types and not necessarily for precise individual weights. We therefore adopted the following procedure to obtain the revised mean types. For any RC2 galaxy having a high-weight type ($w>2.6$) and not based on a PSS print, we adopted the RC2 full type and stage as is with the following exceptions. It was clear from many comparisons that sources S030V and S030C (i.e., from Mount Stromlo 30 in. reflector plates) provided types of quality no better really than a sky survey type, therefore, we treated such types in the same manner as sky survey types. For other large-reflector RC2 types the reduced mean error of 0.30 was used, but for sources B, C, U, E, F, r, S, and all other PSS sources in RC2, we adopted the average reduced mean error $\sigma=0.7$ as a reasonable indication of the uncertainty of such types for what each source considered to be reliable types (that is, not : or ?). For non-PSS types in Hercules, we adopted a reduced mean error of $\sigma_H=0.35$, which at least approximately allows for the nearly factor of four improvement in image scale over sky survey images.

The final procedure was as follows: for all sources except R and S, we set $w_i=1.00$, 0.50, and 0.25 for best, ":", and "?" T values, respectively, while for source S we use the type weight given in the SGC. Then we calculated the mean error for a given source from Eq. (6), the weight from Eq. (7), and the mean type and its mean error from

TABLE 3. Source counts in RC3.

n_S	n_G
1	14 814
2	2 655
3	377
4	59
5	6

Notes to TABLE 3

n_S=number of different sources of types; n_G=number of galaxies in RC3 with mean types based on n_S sources.

Eq. (8). As before, if the mean error comes out less than 0.3 ($w > 10.0$), then the error was fixed at 0.3. Note that for those galaxies lacking an estimate of diameter and axis ratio, we assumed values of log $D_{25}=1.0$ and log $R_{25}=0.2$ for the weight calculation. These are reasonable averages since it is mainly the smaller galaxies that are lacking this information. When the diameters and axis ratios do become available, we could revise the mean types and errors accordingly, but since we round off to the nearest 0.1 in $\langle T \rangle$ and its mean error, we do not expect the revised values to differ very much from those derived now.

4. MEAN FULL TYPES

The problem of computing mean full types (including family and variety parameters) was similar to that of the mean stage index. Our approach was as follows. First, no comparisons were made between family and variety estimates for the sources because these parameters possess a very small range. Secondly, it was with regret that we ignored underlines [e.g., like SA<u>B</u>(r<u>s</u>); see de Vaucouleurs (1963)] because they were not available in all typed versions of our lists. Thus all mean families and varieties were rounded to nearest types, i.e., r, rs, or s, and A, AB, or B.

All sources had full types available on the revised system, but the UGC had these for only a limited subset of 1850 galaxies (out of 12 913). For UGC galaxies lacking a standard full type, we read the Hubble–Sandage type in column (8) of the UGC to at least get an estimate of the family, treating types like Sb/SBb as SABb. To get mean families and varieties we read the uncoded full type for each estimate of full type available, and assigned numerical indices to them in the same manner as de Vaucouleurs & Buta (1980) and Buta & de Vaucouleurs (1982). For family we used $f=-1$ for SA, $f=0$ for SAB, and $f=1$ for SB types, while for variety we used $v=-1$ for (r), $v=0$ for (rs), and $v=1$ for (s).

TABLE 4. Completeness fraction with log D_{25}.

logD$_{25}$	N	n	n/N	logD$_{25}$	N	n	n/N
0.05	0	0	0.00	1.55	447	439	0.98
0.15	7	2	0.29	1.65	234	232	0.99
0.25	18	4	0.22	1.75	140	140	1.00
0.35	35	4	0.11	1.85	64	64	1.00
0.45	43	7	0.16	1.95	39	39	1.00
0.55	159	44	0.28	2.05	23	23	1.00
0.65	257	52	0.20	2.15	13	13	1.00
0.75	405	98	0.24	2.25	8	8	1.00
0.85	975	291	0.30	2.35	7	7	1.00
0.95	2711	1657	0.61	2.45	5	5	1.00
1.05	5921	4914	0.83	2.55	2	2	1.00
1.15	5352	4829	0.90	2.65	1	0	0.00
1.25	2466	2361	0.96	2.75	0	0	0.00
1.35	1587	1527	0.96	2.85	1	1	1.00
1.45	688	675	0.98	2.95	0	0	0.00

Notes to TABLE 4

logD$_{25}$ = center of histogram bin; N = number of RC3 galaxies contained within that bin; n = number of galaxies having a stage index T in that bin

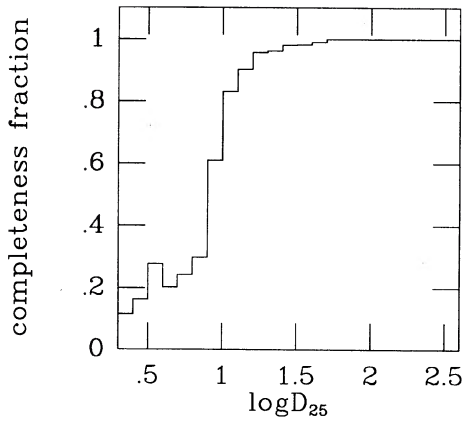

FIG. 4. The fraction of galaxies with available log D_{25} in RC3 having a type T estimate vs log D_{25}, in bins of 0.1 width.

In addition, we read the uncertainty symbols on f and v, that is, as in SA?(rs:)bc, and used these to assign a weight to the parameter estimates. Since RC2 and SGC types do not give the uncertainties on these parameters, but instead provide a general uncertainty symbol which is the "most uncertain" symbol used, we were not able to give separate weights to family and variety based on these symbols. Instead, we computed general uncertainties in the same manner as for the other sources. That is, for a type such as SA?(rs:)bc in ESGC or SA(r)bc? in SGC, the general uncertainty is "?" and the adopted weight for family and variety is 0.25. For a case such as SA(rs:)bc in ESGC or SA(r)bc: in RC2, the general uncertainty is ":" and the f and v weight is 0.50. Otherwise, the f and v weight is 1.0. However, for SGC full types based on more than one estimate, we used instead the SGC type weight because this allowed us to take into account that some SGC types are really means of several estimates and therefore probably deserve somewhat higher weight than indicated by the general uncertainty. We checked the results of this procedure on every galaxy in the final catalogue and we believe it to be quite reasonable.

The mean family and variety were then calculated, but note that if the plate material of a given source did not allow an estimate of family or variety, while others did, we simply averaged the estimates that were given. That is, if six type estimates did not give variety, but one did, then a mean variety is still calculated based on the one estimate. If the mean family $\langle f \rangle$ was from -1.0 to -0.51, we assigned a final family of "A"; if from -0.50 to $+0.50$, we assigned "AB"; and if from $+0.51$ to $+1.0$, we assigned "B". Similarly, if $\langle v \rangle$ was from -1.0 to -0.51, we as-

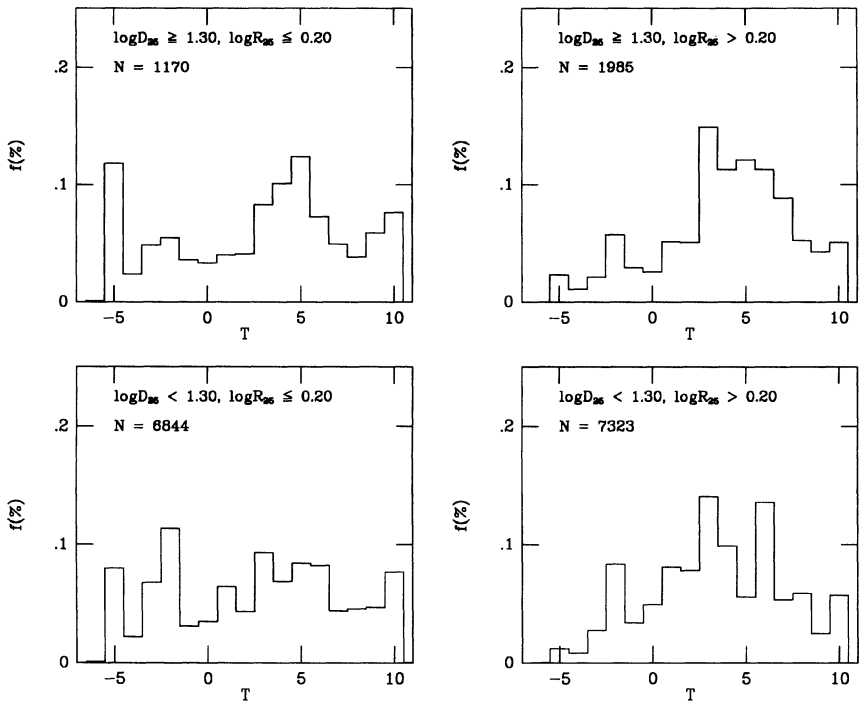

FIG. 5. Distribution of revised Hubble types T for four samples restricted by diameter D_{25} and axis ratio R_{25}.

signed a final variety of "(r)"; if from −0.50 to +0.50, we assigned "(rs)"; and if from +0.51 and +1.0, we assigned "(s)". Note that for galaxies having RC2 types of high weight, we adopted the family and variety from that type estimate alone, rather than averaging it with the sky survey types.

We also computed a "mean outer ring" estimate by assigning an index 0.0 to (R′) and 1.0 to (R). The outer ring was rounded off to (R′) if the mean index was between 0.0 and 0.5, and to (R) if greater than 0.51. Uncertainty symbols were taken into account where relevant.[4]

Finally, any specifications of "pec" or "sp" (for peculiar and spindle, respectively) were read and a numerical symbol assigned. Special cases, e.g., Pec, I0, cI, dE, S pec, etc., were treated as well. All numerical symbols were retained and used to compute a coded mean full type in RC2 style. The final *Revised Mean Type Catalogue* contains 20 074 galaxies, of which 17 911 are entered into RC3. We thoroughly checked every object in the catalogue for identification errors, programming errors, and errors in all of the input type source files. Nevertheless, a few mistakes were identified in the printed version of RC3 and were corrected in Appendix 9 of Vol. I of RC3; this list includes objects that were in the RMTC twice with different names and whose positions failed to agree within the tolerance of 1′.75. We also corrected RC2 types where relevant revisions had been recorded in de Vaucouleurs' copy of RC2, and types based on Buta's 4 m prime focus plates of ringed galaxies. These galaxies are identified as sources "*V*" and "4" in RC3.

Finally, we give in column 2 of Table 2 the number of galaxies having types from each source that were used in the final version of RC3. In Table 3 we also compile the number of galaxies n_G having n_S stage estimates that were averaged into the published mean stage index. Of 17 911 types, 83% are based on only one source, including 1348 objects for which the RC2 type was adopted even when other sources were available. Among these single-source objects are also included galaxies where one source provided two or more estimates. This was common in sources S, E, and F.

5. ANALYSIS

With a set of homogeneous type classifications, we can now examine the distribution of morphologies in the RMTC as well as the type dependence of various objectively measured parameters, such as the integrated colors, mean effective surface brightness, and the hydrogen index. For these purposes, we used revised machine version 9 of RC3, denoted RC3.9a.[5]

[4]The procedure failed for the galaxy IC 2006, which has many type estimates as an E galaxy but in SGC a very faint outer ring was noted (see Schweizer *et al.* 1987). This ring was lost in the printed version of RC3, but has been reinstated into the machine version of RC3 called RC3.9a.

[5]The printed version of RC3 is based on RC3.7. Successive revisions, RC3.8 and RC3.9, had limited distributions; the latest revision, RC3.9a, was made available for distribution by the Data Centers in early 1993.

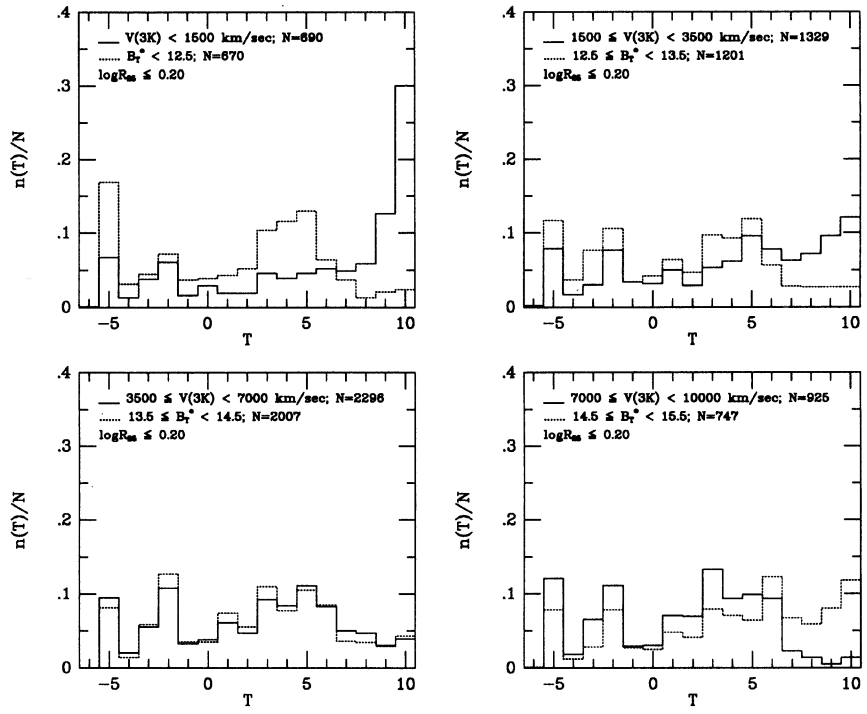

FIG. 6. Distribution of revised Hubble types T for several magnitude-limited and volume-limited samples. The histograms are restricted to galaxies having log $R_{25} \leqslant 0.20$ to minimize classification errors caused by high inclination.

5.1 Completeness Fraction of Catalogue

Figure 4 (see also Table 4) illustrates the completeness fraction of types in RC3 as a function of isophotal diameter log D_{25}. The completeness fraction is the ratio of the number of galaxies having an available estimate of T in a given bin interval of log D_{25}, to the total number of galaxies in that same interval. The fraction is larger than 90% for galaxies having log $D_{25} > 1.2$ ($D_{25} > 1'.6$). Types T are available for the majority of galaxies in RC3 larger than $D_{25} = 1'$, the nominal diameter completeness limit of the catalogue.

5.2 Frequency Function of Types

Figure 5 shows the relative frequency distribution of types in RC3.9a, restricted to certain ranges of diameter and axis ratio. For galaxies of relatively low inclination (log $R_{25} \leqslant 0.20$), the main difference evident between the large and small galaxy samples ($D_{25} \geqslant 2'$ and $D_{25} < 2'$) is a greater relative frequency of S0's in the latter objects. A similar difference is seen among the highly inclined galaxies. Since the relative frequency of intermediate stage spirals is lower among the smaller objects, it is probable that some of the excess S0's ($T = -2$) are misclassified spirals. This is reasonable since most of the types of the smaller galaxies in RC3 are based on sky survey images.

In Fig. 6 (see also Table 5) we show the frequency function of types for four intervals of total magnitude and radial velocity, restricted to log $R_{25} \leqslant 0.20$. These plots highlight selection effects in the type distribution. The volume-limited sample in the upper left panel clearly emphasizes late-type Magellanic spirals and irregulars and highlights the rather low frequency of early-type spirals (types S0/a to Sab). Types Sb to Sdm are virtually equally frequent and comparable in frequency to E's and S0's. However, the comparable-sized magnitude-limited sample clearly emphasizes ellipticals and intermediate to late-type

TABLE 5. Distribution of types.

	V(3K) < 1500 km s^{-1}		B_T^o < 12.5	
T	n(T)	n(T)/N	n(T)	n(T)/N
−6	1	0.001	1	0.001
−5	46	0.067	113	0.169
−4	9	0.013	21	0.031
−3	26	0.038	30	0.045
−2	42	0.061	48	0.072
−1	11	0.016	25	0.037
0	20	0.029	26	0.039
1	13	0.019	29	0.043
2	13	0.019	35	0.052
3	32	0.046	70	0.104
4	27	0.039	78	0.116
5	32	0.046	87	0.130
6	36	0.052	43	0.064
7	34	0.049	25	0.037
8	41	0.059	9	0.013
9	87	0.126	14	0.021
10	207	0.300	16	0.024
11	1	0.001	–	–
90	6	0.009	–	–
99	6	0.009	–	–

Notes to TABLE 5

Counts restricted to logR$_{25} \leq 0.20$. For radial velocity-limited sample, N = 690. For magnitude-limited sample, N = 670. Types T = 90 and 99 correspond to I0 and Pec classifications, respectively, in RC3. None of these is included in the magnitude-limited sample since such galaxies cannot be reliably corrected for inclination.

TABLE 6. Mean total colors by type.

T	$<(B-V)^0_T>$	σ	N	$<(U-B)^0_T>$	σ	N	$(B-V)^0_T$ median	$(U-B)^0_T$ median
−5	0.915	0.042	282	0.490	0.066	203	0.92	0.49
−4	0.907	0.042	85	0.461	0.092	62	0.91	0.47
−3	0.909	0.049	185	0.467	0.089	127	0.91	0.48
−2	0.894	0.060	265	0.447	0.097	222	0.90	0.46
−1	0.885	0.056	96	0.422	0.110	83	0.89	0.42
0	0.812	0.104	95	0.316	0.165	82	0.82	0.34
1	0.742	0.103	146	0.222	0.154	114	0.76	0.24
2	0.717	0.098	116	0.177	0.147	92	0.73	0.20
3	0.605	0.112	267	0.050	0.130	203	0.61	0.06
4	0.566	0.097	258	−0.029	0.116	189	0.57	−0.03
5	0.526	0.103	322	−0.075	0.111	180	0.53	−0.08
6	0.472	0.100	132	−0.138	0.104	96	0.47	−0.14
7,8	0.499	0.086	108	−0.125	0.115	84	0.50	−0.13
9	0.449	0.087	90	−0.165	0.126	86	0.43	−0.17
10	0.421	0.110	142	−0.216	0.138	135	0.41	−0.23

TABLE 7. Mean effective colors by type.

T	$<(B-V)^0_e>$	σ	N	$<(U-B)^0_e>$	σ	N	$(B-V)^0_e$ median	$(U-B)^0_e$ median
−5	0.941	0.034	257	0.533	0.058	180	0.94	0.54
−4	0.938	0.039	76	0.517	0.070	50	0.95	0.52
−3	0.935	0.043	153	0.513	0.075	108	0.94	0.51
−2	0.928	0.053	204	0.490	0.086	173	0.94	0.51
−1	0.915	0.051	82	0.463	0.106	71	0.92	0.47
0	0.857	0.072	66	0.377	0.113	57	0.87	0.39
1	0.792	0.099	103	0.268	0.154	85	0.81	0.30
2	0.785	0.084	88	0.279	0.132	66	0.80	0.30
3	0.695	0.092	197	0.133	0.134	161	0.70	0.14
4	0.629	0.093	218	0.041	0.118	151	0.64	0.05
5	0.593	0.096	243	−0.009	0.120	135	0.60	−0.01
6	0.516	0.095	90	−0.098	0.099	66	0.52	−0.08
7,8	0.524	0.081	74	−0.104	0.111	59	0.52	−0.12
9	0.458	0.078	74	−0.129	0.101	69	0.47	−0.12
10	0.394	0.112	116	−0.208	0.127	108	0.39	−0.21

spirals (types Sb to Sc), with Magellanic spirals and irregulars having the lowest frequencies. These distributions compare favorably with Fig. 3 of de Vaucouleurs (1963). Table 5 lists the frequencies only for these two samples. The remaining panels in Fig. 6 show the progressive loss of Magellanic spirals and irregulars with increasing distance and the increasing abundance of these types at fainter magnitudes.

5.3 The Revised Hubble Sequence and Measured Parameters

The correlations between revised Hubble types and integrated colors, and similar correlations for mean surface brightness, hydrogen index, and bulge-to-disk ratio, are the main evidence for a physical significance to the Hubble sequence. These correlations were first documented with RC2 data by de Vaucouleurs (1977). It is worth reexamining them using the more precise and much enlarged database in RC3. We initially use unrestricted samples to see the basic correlations provided by the whole catalogue, and then we apply restrictions according to galactic latitude, radial velocity, and inclination. However, before discussing the colors, we must point out an error in the printed version (RC3.7) of RC3 that would cause confusion since we have used parameters from machine version RC3.9a in this paper that differ from the printed values.

5.3.1 The error in the corrected colors of RC3.7

After the printed version of RC3 was published, we discovered an unfortunate error in the computation of the corrected color indices $(B-V)^0_T$ and $(U-B)^0_T$.[6] As printed, these colors are corrected for inclination (internal absorption effect) using the procedure outlined by Eqs. (24), (32), (33), and (35) of RC2. However, the Introduction to RC3, Sec. 3.7.b, Eqs. (63) and (64), states that a very different procedure was used. Corrected colors computed according to the Introduction to RC3 on average (over all types) differ negligibly from those corrected according to RC2 procedures. However, in individual cases, the differences can amount to as much as 0.2 mag, especially for late-type magellanic irregulars and spirals. The corrected color indices in machine version RC3.9a are recomputed using the intended RC3 procedure. As we show below, even this procedure may need revision at some point.

The inclination corrections in RC3 are perhaps the most contentious and all astronomers should be aware of their uncertainties. A detailed discussion and justification of those outlined in the Introduction to RC3 will be presented elsewhere. We note that the *observed* colors $(B-V)_T$, $(U-B)_T$, $(B-V)_e$, and $(U-B)_e$ are *not* at issue here and that some astronomers may prefer another recipe for correcting these colors for inclination.

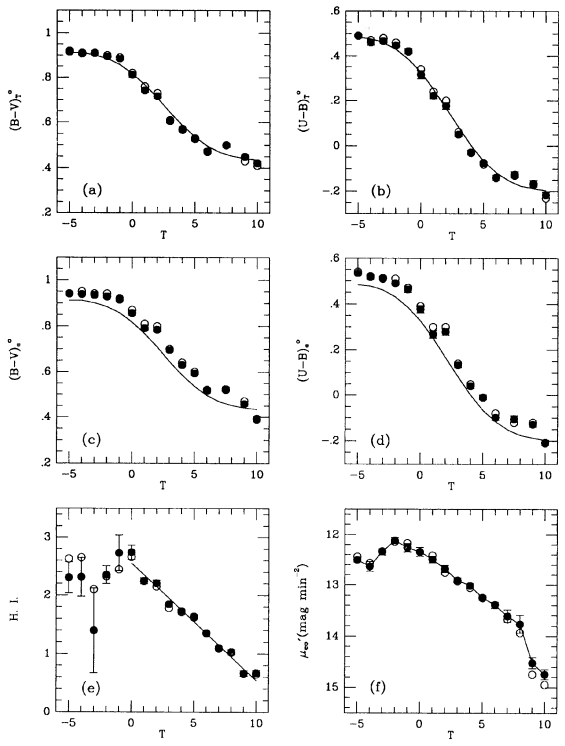

FIG. 7. Type correlations for samples of RC3 galaxies (see Tables 6–8). Filled circles are means and open circles are medians. The curves in (a) and (b) are integral Gaussian functions that approximate the dependence of the corrected total colors on type. The curves are not intended as a physical explanation of this dependence. The curves in (c) and (d) are the same as in (a) and (b) to highlight how effective colors differ from total colors. The line in (e) is based on Eq. (14).

[6]A more complete errata list is provided in Corwin *et al.* (1994).

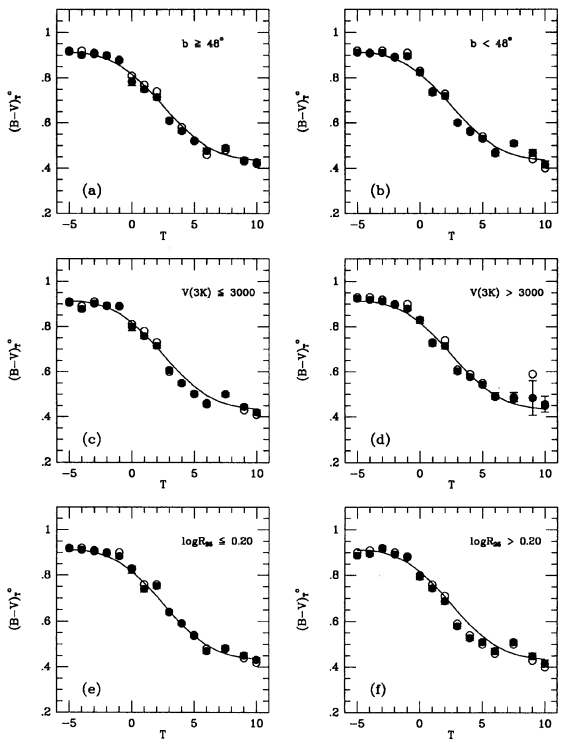

FIG. 8. Type correlations for $(B-V)_T^0$ colors for samples divided by galactic latitude b, corrected radial velocity with respect to the microwave background, $V(3K)$, and logarithmic axis ratio $\log R_{25}$.

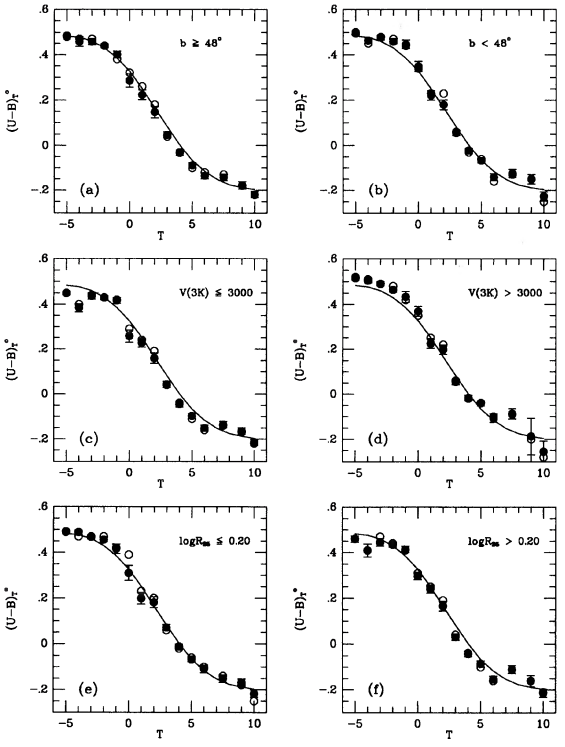

FIG. 9. Same as Fig. 8 for $(U-B)_T^0$ colors.

5.3.2 Type correlations

Because of problems with bright emission lines in some early-type galaxies, it was necessary to do a rejection sequence for the mean colors for each type, rather than simply taking averages. The sequence began with one cycle of 2σ rejection, followed by single cycles of 2.25σ and 2.5σ rejection, and ending with two final cycles of 2.75σ rejection. After the rejection sequence, final means and medians for both total and effective colors were computed. These are compiled in Tables 6 and 7 and illustrated in Figs. 7(a)–7(d). We have combined types 7 and 8 (Sd and Sdm) in these plots since the samples in each category alone would be small. A very good monotonic relationship with type is evident in each color. Laplace–Gauss integrals provide a good description of the relationships for the total

TABLE 8. Mean hydrogen index and surface brightness by type.

T	< *H.I.* >	σ	N	$< \mu'_{eo} >$	σ	N	*H.I.* median	μ'_{eo} median
−5	2.302	0.935	12	12.500	0.705	268	2.63	12.44
−4	2.312	0.668	4	12.630	0.833	75	2.65	12.56
−3	1.395	1.453	4	12.341	0.811	155	2.10	12.33
−2	2.350	1.058	46	12.115	0.868	209	2.32	12.14
−1	2.730	1.343	19	12.256	0.761	85	2.44	12.17
0	2.740	1.123	79	12.340	0.720	68	2.66	12.34
1	2.243	0.818	222	12.494	0.633	102	2.24	12.41
2	2.205	0.756	219	12.677	0.673	86	2.15	12.76
3	1.844	0.631	534	12.903	0.681	204	1.78	12.93
4	1.728	0.564	425	13.014	0.594	219	1.71	13.05
5	1.638	0.518	413	13.241	0.585	238	1.62	13.25
6	1.352	0.531	527	13.394	0.569	87	1.35	13.39
7	1.097	0.527	265	13.606	0.794	41	1.09	13.66
8	1.030	0.596	232	13.766	0.972	32	1.02	13.93
9	0.663	0.636	180	14.520	0.942	76	0.66	14.75
10	0.672	0.776	286	14.748	1.062	114	0.65	14.95

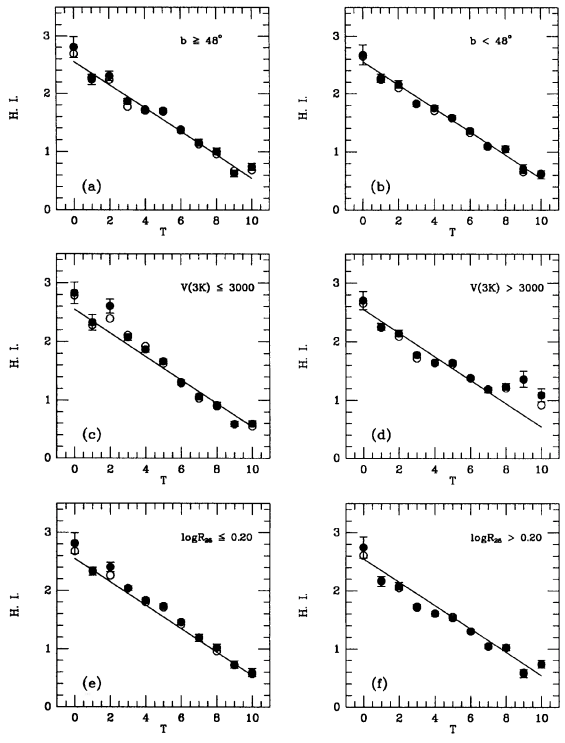

FIG. 10. Same as Fig. 8 for hydrogen indices.

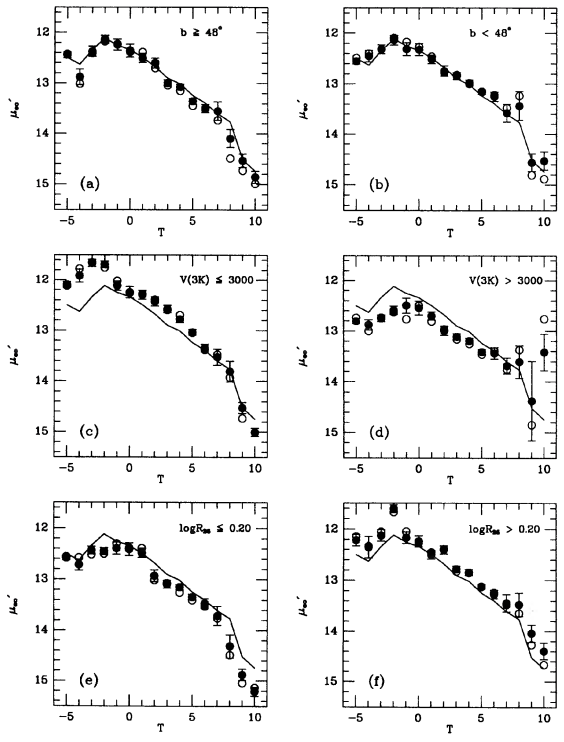

FIG. 11. Same as Fig. 8 for mean surface brightnesses.

colors, and the same curves are plotted on the graphs for the effective colors to highlight the average differences between effective and integrated colors. These relationships are similar to those found by de Vaucouleurs (1977), but there are important differences. The colors in RC3.9 are corrected for galactic and internal extinction using the Burstein–Heiles model and completely different inclination corrections.

The mean effective surface brightness, m'_e, is derived from photoelectric aperture photometry and represents the surface brightness within the (circular) *effective* aperture, A_e, which transmits half the total B-band flux. This differs from the mean surface brightness, μ'_e, within the *equivalent* effective diameter, $r_e = \sqrt{a_e b_e}$, by an amount depending on the inclination of the galaxy. Olson & de Vaucouleurs (1981) showed that for a pure exponential disk or an $r^{1/4}$ law, the correction can be approximated by

$$\mu'_e = m'_e - 1.3(\log R_{25})^2. \quad (12)$$

From this we also subtract the galactic extinction correction $A_g(B)$ as listed in RC3.9.

Finally, the hydrogen index is defined in RC3 as

$$\text{H.I.} = m^0_{21} - B^0_T, \quad (13)$$

where m^0_{21} is the corrected 21 cm magnitude and B^0_T is the corrected total B-band magnitude. From this parameter, the hydrogen mass-to-blue luminosity ratio can be estimated using Eq. (78) in the Introduction to RC3.[7]

[7]This equation is missing a minus sign in the printed catalogue. The correct equation is $\log(\mathbf{M}_H/L^0_B)_\odot = -0.4\text{HI} + 0.4[M_B(\odot) - 5.46]$.

TABLE 9. Mean total colors by type and galactic latitude.

T	$<(B-V)^0_T>$	σ	N	$<(U-B)^0_T>$	σ	N	$(B-V)^0_T$ median	$(U-B)^0_T$ median
				$b \geq 48°$				
−5	0.915	0.038	138	0.485	0.065	104	0.92	0.48
−4	0.902	0.046	31	0.458	0.101	21	0.92	0.47
−3	0.906	0.051	84	0.457	0.095	56	0.91	0.47
−2	0.897	0.054	143	0.439	0.095	121	0.90	0.44
−1	0.877	0.053	47	0.401	0.097	44	0.88	0.38
0	0.784	0.127	51	0.286	0.190	44	0.81	0.32
1	0.750	0.105	73	0.224	0.162	57	0.77	0.26
2	0.714	0.101	58	0.147	0.167	45	0.74	0.18
3	0.611	0.112	127	0.047	0.132	98	0.61	0.04
4	0.564	0.101	134	−0.033	0.122	99	0.58	−0.03
5	0.522	0.087	143	−0.088	0.106	81	0.52	−0.10
6	0.476	0.113	71	−0.135	0.095	47	0.46	−0.12
7,8	0.489	0.091	64	−0.142	0.102	46	0.48	−0.13
9	0.435	0.096	59	−0.178	0.128	55	0.43	−0.18
10	0.425	0.110	85	−0.219	0.121	77	0.42	−0.22
				$b < 48°$				
−5	0.911	0.051	149	0.495	0.068	99	0.92	0.50
−4	0.908	0.042	55	0.463	0.080	39	0.91	0.45
−3	0.910	0.050	102	0.476	0.083	71	0.92	0.48
−2	0.893	0.075	126	0.459	0.095	100	0.89	0.47
−1	0.895	0.055	48	0.446	0.120	39	0.91	0.44
0	0.824	0.084	45	0.348	0.136	38	0.83	0.34
1	0.734	0.102	73	0.221	0.160	59	0.74	0.23
2	0.719	0.096	58	0.180	0.153	50	0.73	0.23
3	0.601	0.115	141	0.056	0.125	104	0.60	0.06
4	0.565	0.096	126	−0.022	0.102	87	0.56	−0.03
5	0.530	0.112	176	−0.067	0.112	98	0.54	−0.06
6	0.465	0.088	62	−0.141	0.113	49	0.47	−0.16
7,8	0.509	0.073	43	−0.125	0.111	35	0.51	−0.13
9	0.468	0.078	32	−0.151	0.114	30	0.44	−0.15
10	0.416	0.110	57	−0.227	0.147	55	0.40	−0.25

The dependences of the mean surface brightness and hydrogen index on type were computed in the same manner as for the colors, i.e., with a staggered rejection sequence. The results are compiled in Table 8 and illustrated in Figs. 7(e) and 7(f). The hydrogen index depends linearly on T for spirals ($T \geqslant 0$), with the following impartial relation:

$$\text{H.I.} = 1.53 - (0.204 \pm 0.016)(T - 5.38). \quad (14)$$

A clear correlation between mean surface brightness and type is also evident for the spirals and S0's. The plot sug-

TABLE 10. Mean total colors by type and radial velocity.

T	$<(B-V)^0_T>$	σ	N	$<(U-B)^0_T>$	σ	N	$(B-V)^0_T$ median	$(U-B)^0_T$ median
				V(3K) ≤ 3000 km s^{-1}				
−5	0.904	0.038	113	0.449	0.073	95	0.91	0.45
−4	0.877	0.041	24	0.384	0.081	21	0.89	0.40
−3	0.901	0.047	65	0.436	0.107	60	0.91	0.44
−2	0.893	0.061	115	0.429	0.091	103	0.89	0.43
−1	0.888	0.052	54	0.416	0.095	52	0.89	0.42
0	0.798	0.112	52	0.257	0.194	48	0.81	0.29
1	0.758	0.105	72	0.227	0.142	55	0.78	0.24
2	0.715	0.087	50	0.159	0.147	41	0.73	0.19
3	0.607	0.107	110	0.043	0.145	100	0.60	0.04
4	0.549	0.098	113	−0.046	0.110	91	0.55	−0.04
5	0.503	0.100	142	−0.097	0.113	106	0.50	−0.11
6	0.456	0.090	80	−0.151	0.099	58	0.46	−0.16
7,8	0.499	0.081	82	−0.136	0.111	60	0.50	−0.14
9	0.445	0.079	84	−0.164	0.123	81	0.43	−0.17
10	0.421	0.110	126	−0.213	0.128	116	0.41	−0.22
				V(3K) > 3000 km s^{-1}				
−5	0.923	0.044	169	0.514	0.057	111	0.93	0.52
−4	0.918	0.039	62	0.504	0.059	38	0.93	0.51
−3	0.912	0.052	121	0.491	0.072	67	0.92	0.49
−2	0.896	0.059	149	0.464	0.097	118	0.90	0.48
−1	0.880	0.063	42	0.433	0.132	31	0.90	0.42
0	0.828	0.095	43	0.369	0.130	36	0.83	0.35
1	0.726	0.100	74	0.225	0.171	60	0.73	0.25
2	0.714	0.111	67	0.197	0.142	50	0.74	0.22
3	0.602	0.122	160	0.054	0.119	104	0.61	0.06
4	0.577	0.097	146	−0.016	0.118	97	0.59	−0.02
5	0.543	0.099	177	−0.041	0.098	73	0.55	−0.04
6	0.493	0.108	51	−0.106	0.119	40	0.49	−0.10
7,8	0.488	0.100	25	−0.087	0.112	23	0.48	−0.09
9	0.484	0.170	5	−0.188	0.182	5	0.59	−0.20
10	0.457	0.148	18	−0.255	0.197	18	0.45	−0.28

TABLE 11. Mean total colors by type and inclination.

T	$<(B-V)^0_T>$	σ	N	$<(U-B)^0_T>$	σ	N	$(B-V)^0_T$ median	$(U-B)^0_T$ median
				$\log R_{25} \leq 0.20$				
−5	0.918	0.041	237	0.492	0.068	171	0.92	0.49
−4	0.912	0.039	63	0.488	0.062	43	0.92	0.47
−3	0.905	0.054	125	0.467	0.087	85	0.91	0.47
−2	0.896	0.058	146	0.456	0.094	115	0.90	0.47
−1	0.884	0.069	44	0.416	0.133	41	0.90	0.42
0	0.825	0.118	53	0.310	0.226	46	0.83	0.39
1	0.739	0.108	62	0.199	0.179	52	0.76	0.23
2	0.753	0.081	53	0.181	0.152	41	0.76	0.20
3	0.640	0.105	110	0.071	0.115	79	0.64	0.06
4	0.592	0.088	142	−0.012	0.107	90	0.59	−0.02
5	0.536	0.104	191	−0.067	0.091	86	0.54	−0.06
6	0.471	0.092	59	−0.108	0.097	34	0.48	−0.10
7,8	0.482	0.073	46	−0.151	0.105	37	0.48	−0.14
9	0.451	0.090	56	−0.168	0.121	55	0.44	−0.18
10	0.432	0.091	76	−0.217	0.139	73	0.42	−0.25
				$\log R_{25} > 0.20$				
−5	0.887	0.049	47	0.459	0.084	36	0.90	0.46
−4	0.895	0.049	22	0.409	0.107	14	0.91	0.41
−3	0.917	0.039	60	0.445	0.117	46	0.92	0.47
−2	0.892	0.063	119	0.434	0.101	108	0.90	0.44
−1	0.884	0.046	52	0.415	0.090	42	0.88	0.41
0	0.795	0.083	42	0.297	0.102	38	0.80	0.31
1	0.744	0.101	84	0.240	0.143	64	0.76	0.25
2	0.688	0.100	62	0.166	0.152	52	0.71	0.19
3	0.579	0.111	156	0.030	0.151	129	0.59	0.04
4	0.527	0.105	119	−0.042	0.112	94	0.54	−0.04
5	0.510	0.103	132	−0.086	0.131	95	0.50	−0.10
6	0.471	0.104	72	−0.152	0.103	61	0.46	−0.16
7,8	0.509	0.086	59	−0.110	0.117	46	0.50	−0.11
9	0.448	0.084	34	−0.161	0.137	31	0.43	−0.16
10	0.416	0.125	64	−0.214	0.138	62	0.40	−0.21

TABLE 13. Mean hydrogen index and surface brightness by type and radial velocity.

T	$<H.I.>$	σ	N	$<\mu'_{eo}>$	σ	N	$H.I.$ median	μ'_{eo} median
				$V(3K) \leq 3000$ km s^{-1}				
−5	2.032	0.912	9	12.096	0.638	118	2.01	12.12
−4	2.312	0.668	4	11.917	0.584	20	2.65	11.77
−3	1.113	1.640	3	11.661	0.576	61	2.02	11.65
−2	2.511	1.286	17	11.692	0.701	102	2.25	11.76
−1	3.461	1.546	8	12.113	0.686	53	3.49	12.02
0	2.828	1.250	46	12.245	0.741	42	2.79	12.26
1	2.327	1.169	75	12.298	0.675	57	2.28	12.28
2	2.604	0.983	64	12.431	0.594	43	2.39	12.40
3	2.073	0.736	159	12.579	0.689	94	2.11	12.60
4	1.867	0.639	154	12.785	0.610	100	1.92	12.70
5	1.666	0.558	201	13.037	0.590	110	1.63	13.05
6	1.309	0.579	200	13.347	0.574	58	1.29	13.39
7	1.062	0.545	157	13.531	0.907	33	1.03	13.47
8	0.919	0.611	148	13.810	1.015	25	0.90	13.93
9	0.592	0.604	163	14.526	0.935	73	0.59	14.73
10	0.598	0.799	257	15.004	0.794	97	0.55	15.01
				$V(3K) > 3000$ km s^{-1}				
−5	1.850	2.543	4	12.806	0.629	150	3.29	12.74
−4	–	–	–	12.878	0.760	54	–	13.00
−3	2.240	–	1	12.750	0.632	91	2.24	12.74
−2	2.255	0.911	29	12.590	0.853	108	2.32	12.63
−1	2.553	1.508	12	12.498	0.840	32	2.44	12.77
0	2.703	0.879	32	12.545	0.712	27	2.65	12.49
1	2.255	0.726	150	12.703	0.543	46	2.24	12.81
2	2.142	0.730	162	12.995	0.587	41	2.09	12.97
3	1.773	0.595	380	13.113	0.628	112	1.72	13.16
4	1.649	0.509	270	13.193	0.518	118	1.64	13.25
5	1.641	0.521	219	13.414	0.514	126	1.62	13.46
6	1.386	0.507	329	13.439	0.611	30	1.38	13.40
7	1.180	0.487	107	13.686	0.474	9	1.19	13.76
8	1.237	0.513	83	13.608	0.850	7	1.21	13.37
9	1.365	0.568	17	14.377	1.352	3	1.36	14.85
10	1.091	0.616	32	13.420	1.345	14	0.92	12.76

gests that a typical elliptical has a lower average surface brightness than an S0, but this difference becomes less significant when the comparison is restricted to S0's having low inclinations, as we now show.

To highlight some of the biases and uncertainties in these relations, we have computed the type correlations for the total colors, the hydrogen index, and the mean effective surface brightness for the following samples: (1) galactic latitude $b \geqslant 48°$ and $b < 48°$; (2) corrected radial velocity $V(3K) \leqslant 3000$ km s^{-1} and $V(3K) > 3000$ km s^{-1}; and (3) logarithmic axis ratio $\log R_{25} \leqslant 0.20$ and $\log R_{25} > 0.20$. The divisions are the rough medians for the color samples. Figures 8–11 (see Tables 9–14) illustrate the type correlations for the divided samples. The solid curves or lines in each case are based on the full samples illustrated in Fig. 7, and are intended only for reference to those samples. For each of the four illustrated parameters, there appears to be little dependence on galactic latitude. However, significant differences are found for the radial velocity and inclination

TABLE 12. Mean hydrogen index and surface brightness by type and galactic latitude.

T	$<H.I.>$	σ	N	$<\mu'_{eo}>$	σ	N	$H.I.$ median	μ'_{eo} median
				$b \geq 48°$				
−5	2.476	0.811	8	12.448	0.678	130	2.93	12.43
−4	1.755	0.007	2	12.881	0.820	27	1.76	13.02
−3	1.113	1.640	3	12.373	0.856	70	2.02	12.40
−2	2.562	1.027	20	12.135	0.836	111	2.32	12.18
−1	2.821	1.027	8	12.237	0.712	43	3.06	12.23
0	2.807	1.160	39	12.355	0.771	37	2.69	12.39
1	2.245	0.870	94	12.503	0.658	51	2.28	12.39
2	2.307	0.794	93	12.601	0.620	40	2.24	12.70
3	1.867	0.640	233	12.997	0.578	85	1.77	13.04
4	1.702	0.509	202	13.073	0.556	107	1.72	13.15
5	1.705	0.495	181	13.353	0.593	105	1.69	13.45
6	1.365	0.480	222	13.498	0.552	45	1.38	13.51
7	1.157	0.603	110	13.552	0.902	24	1.13	13.73
8	1.007	0.584	103	14.101	0.763	18	0.96	14.49
9	0.629	0.608	102	14.537	0.922	47	0.67	14.73
10	0.744	0.733	156	14.859	0.923	63	0.69	14.99
				$b < 48°$				
−5	1.176	2.021	5	12.549	0.709	136	0.97	12.49
−4	2.870	0.311	2	12.453	0.783	47	3.09	12.40
−3	2.240	–	1	12.314	0.777	85	2.24	12.31
−2	2.287	1.174	27	12.135	0.979	102	2.25	12.09
−1	2.664	1.580	11	12.313	0.845	43	2.44	12.17
0	2.675	1.097	40	12.322	0.666	31	2.65	12.27
1	2.273	0.814	130	12.513	0.586	50	2.24	12.46
2	2.162	0.758	128	12.743	0.715	46	2.10	12.78
3	1.821	0.619	300	12.845	0.738	118	1.83	12.82
4	1.754	0.625	225	12.981	0.608	110	1.71	13.00
5	1.590	0.518	229	13.162	0.557	132	1.58	13.15
6	1.360	0.575	307	13.253	0.599	43	1.33	13.22
7	1.087	0.470	155	13.580	0.750	18	1.10	13.47
8	1.047	0.627	131	13.437	1.038	13	1.05	13.24
9	0.709	0.640	76	14.564	0.933	28	0.66	14.81
10	0.611	0.800	128	14.532	1.305	52	0.63	14.89

TABLE 14. Mean hydrogen index and surface brightness by type and inclination.

T	$<H.I.>$	σ	N	$<\mu'_{eo}>$	σ	N	$H.I.$ median	μ'_{eo} median
				$\log R_{25} \leq 0.20$				
−5	2.279	0.974	10	12.584	0.657	220	2.63	12.56
−4	2.870	0.311	2	12.718	0.802	57	3.09	12.58
−3	1.395	1.453	4	12.435	0.811	102	2.10	12.52
−2	2.604	1.063	27	12.452	0.793	122	2.51	12.50
−1	2.906	1.319	11	12.394	0.771	41	3.06	12.31
0	2.813	1.043	33	12.414	0.808	41	2.68	12.39
1	2.332	0.710	105	12.485	0.607	44	2.34	12.39
2	2.404	0.759	86	12.929	0.728	41	2.26	13.01
3	2.039	0.611	214	13.093	0.725	91	2.04	13.08
4	1.832	0.560	203	13.151	0.542	116	1.80	13.25
5	1.733	0.557	250	13.340	0.641	144	1.71	13.41
6	1.459	0.536	207	13.466	0.617	42	1.42	13.52
7	1.188	0.584	95	13.711	0.827	19	1.19	13.76
8	1.023	0.594	102	14.315	0.928	16	0.96	14.49
9	0.730	0.682	112	14.881	0.780	46	0.72	15.05
10	0.591	0.834	157	15.211	0.656	55	0.57	15.14
				$\log R_{25} > 0.20$				
−5	2.415	1.025	2	12.216	0.742	44	3.14	12.15
−4	1.755	0.007	2	12.354	0.895	18	1.76	12.34
−3	–	–	–	12.125	0.816	54	–	12.05
−2	2.133	1.143	20	11.607	0.676	82	2.26	11.67
−1	2.487	1.427	8	12.167	0.777	45	2.34	12.05
0	2.746	1.239	47	12.236	0.582	27	2.61	12.27
1	2.161	0.912	117	12.501	0.657	58	2.17	12.46
2	2.079	0.732	133	12.405	0.521	43	2.05	12.39
3	1.728	0.623	321	12.779	0.614	113	1.71	12.83
4	1.603	0.556	223	12.844	0.607	102	1.61	12.85
5	1.529	0.469	167	13.120	0.439	92	1.55	13.12
6	1.304	0.540	325	13.269	0.578	47	1.30	13.24
7	1.047	0.476	168	13.443	0.832	23	1.04	13.47
8	1.024	0.609	131	13.474	0.920	16	1.02	13.65
9	0.577	0.568	69	14.042	0.894	28	0.59	14.27
10	0.740	0.730	131	14.394	1.219	55	0.74	14.66

TABLE 15. Representative galaxies.

α (2000) δ	Name	logD_{25}	Type	T	Source	$(B-V)^o_T$	$(U-B)^o_T$	H. I.	μ'_{eo}
0042+4051	NGC 221	1.94	cE2	−6.0	R	0.88	0.40	–	9.70
0131−0652	NGC 584	1.62	E4	−5.0	R	0.91	0.47	–	11.30
0335−3513	NGC 1374	1.39	E	−4.5	RBCS	0.91	0.47	–	12.04
0336−3526	NGC 1379	1.38	E	−5.0	RBCS	0.88	0.38	–	12.87
0456−0452	NGC 1700	1.52	E4	−5.0	R	0.91	0.49	–	11.51
1047+1234	NGC 3379	1.73	E1	−5.0	R	0.94	0.52	–	11.26
1109−3732	NGC 3557	1.61	E3	−5.0	R	0.87	0.49	–	11.51
1116+1808	NGC 3608	1.50	E2	−5.0	R	0.93	0.40	6.82	12.47
1231+2546	NGC 4494	1.68	E1+	−5.0	R	0.85	0.44	–	12.17
1253−3942	NGC 4767	1.42	E	−4.5	RBCS	0.91	–	–	11.97
1349+6011	NGC 5322	1.77	E3+	−5.0	R	0.89	0.48	–	11.84
1501+0142	NGC 5813	1.62	E1+	−5.0	R	0.94	0.52	–	13.15
2152−4815	NGC 7144	1.57	E0	−5.0	R	0.90	0.43	–	12.54
0057+3021	NGC 315	1.51	E$^+$:	−4.0	PU	0.93	0.56	–	12.77
0132−0701	NGC 596	1.51	E$^+$p	−4.0	PE	0.86	0.40	–	11.97
0342−3523	NGC 1427	1.56	E$^+$	−4.1	RBCS	0.90	0.43	–	12.31
1036−2731	NGC 3311	1.54	E$^+$2	−4.0	V	0.92	0.55	–	13.20
1204+0153	NGC 4073	1.50	E$^+$	−3.8	PUEF	0.94	–	–	13.86
1230+1223	NGC 4486	1.92	E$^+$0+p	−4.0	R	0.93	0.55	–	12.50
1244−4145	NGC 4645	1.35	E$^+$	−3.6	RBCS	0.91	–	–	11.57
1300+3718	NGC 4914	1.54	E$^+$	−4.0	PU	0.86	0.49	–	12.20
2048−3759	NGC 6958	1.33	E$^+$	−3.8	RBCS	0.86	0.45	–	11.81
0109+3543	NGC 404	1.54	LA(s)0$^-$:	−3.0	R	0.89	0.21	2.45	11.31
0330−3451	NGC 1351	1.45	LA0$^-$p:	−3.0	RBCS	0.87	0.36	–	12.04
0336−3530	NGC 1387	1.45	LAB(s)0$^-$	−3.0	RBCS	0.98	0.51	–	11.55
0338−4406	NGC 1411	1.36	LA(r)0$^-$:	−3.0	RBCS	0.96	0.39	–	10.99
1129−3623	NGC 3706	1.48	LA(rs)0$^-$	−3.0	RBCS	0.93	0.50	–	11.58
1215+3311	NGC 4203	1.53	LAB0$^-$:	−3.0	R	0.93	0.53	2.36	11.44
1219+1247	NGC 4267	1.51	LB(s)0$^-$?	−3.0	R	0.91	0.57	–	12.85
1225−3945	NGC 4373	1.53	LAB0$^-$:	−2.9	PBS	0.86	0.37	–	11.91
1247−4131	NGC 4683	1.16	LB(s)0$^-$	−2.6	RBCS	0.93	0.46	–	12.46
1252+1118	NGC 4754	1.66	LB(r)0$^-$:	−3.0	R	0.90	0.47	–	11.55
2300+3008	NGC 7457	1.63	LA(rs)0$^-$?	−3.0	R	0.83	0.32	–	12.44
2344−4254	NGC 7744	1.34	LAB(s)0$^-$	−2.7	RBCS	0.91	0.51	–	11.12
0304−2604	NGC 1201	1.56	LA(r)0°:	−2.0	R	0.92	0.53	–	11.94
0336−3517	NGC 1381	1.43	LA0: sp	−1.6	RBCS	0.92	0.47	–	10.50
0345−1816	NGC 1440	1.33	(R′)LB(rs)0°:	−1.9	PSEr	0.97	0.57	–	12.33
0416−5546	NGC 1553	1.65	LA(r)0°	−2.0	R	0.87	0.49	3.35	12.08
0933+1009	NGC 2911	1.61	LA(s)0:p	−2.0	R	0.91	0.46	3.47	14.04
1027+2830	NGC 3245	1.51	LA(r)0°:	−2.0	R	0.89	0.47	–	11.80
1050+1324	NGC 3412	1.56	LB(s)0°	−2.0	R	0.89	0.38	–	11.50
1116+1803	NGC 3607	1.69	LA(s)0°:	−2.0	R	0.92	0.49	–	12.03
1241+1009	NGC 4608	1.51	LB(r)0°	−2.0	R	0.95	–	–	–
1848−6510	NGC 6684	1.60	(R′)LB(s)0°	−2.0	R	0.86	0.38	–	11.77
2119−4833	NGC 7049	1.63	LA(s)0°	−2.0	R	1.02	0.58	–	11.70
2322−4228	NGC 7632	1.34	(R′)LB(s)0°:	−2.0	PBSr	0.85	0.33	–	12.73
0227−0109	NGC 936	1.67	LB(rs)0$^+$	−1.0	R	0.95	0.56	4.47	12.31
0341−1816	IC 346	1.31	LB(rs)0$^+$	−0.8	PSEr	0.92	0.51	–	13.71
0621−2714	NGC 2217	1.65	(R)LB(rs)0$^+$	−1.0	R	0.95	0.51	2.34	12.05
0919+6912	NGC 2787	1.50	LB(r)0$^+$	−1.0	R	1.02	0.63	2.71	11.64
0924+3430	NGC 2859	1.63	(R)LB(r)0$^+$	−1.0	R	0.91	0.48	5.58	12.42
1100+1354	NGC 3489	1.55	LAB(rs)0$^+$	−1.0	R	0.82	0.34	6.30	10.67
1153+6040	NGC 3945	1.72	(R)LB(rs)0$^+$	−1.0	Rb	0.92	0.54	–	11.52
1223+1643	NGC 4340	1.55	LB(r)0$^+$	−1.0	R	0.91	0.50	–	13.01
1224+1142	NGC 4371	1.60	LB(r)0$^+$	−1.0	R	0.97	0.56	–	11.73
1225+1811	NGC 4382	1.85	LA(s)0$^+$p	−1.0	R	0.88	0.42	–	11.81
1239+1010	NGC 4596	1.60	LB(r)0$^+$	−1.0	R	0.92	0.51	–	12.38
0243−2900	NGC 1079	1.54	(R)SAB(rs)0/ap	0.0	R	0.87	0.42	1.34	12.26
0317−4106	NGC 1291	1.99	(R)SB(s)0/a	0.0	R	0.91	0.45	3.54	11.62
0319−2603	NGC 1302	1.59	(R)SB(r)0/a	0.0	V	0.87	0.35	2.79	12.39
0340−2233	NGC 1415	1.54	(R)SAB(s)0/a	0.0	R	0.86	0.32	2.70	12.65
0345−1838	NGC 1452	1.35	(R′)SB(r)0/a	0.4	PSEr	0.91	0.53	–	12.62
0855+7813	NGC 2655	1.69	SAB(s)0/a	0.0	R	0.83	0.42	2.60	11.96
0853+5118	NGC 2681	1.56	(R′)SAB(rs)0/a	0.0	R	0.76	0.29	–	11.97
1252−4103	NGC 4744	1.33	SB(s)0/a	−0.3	PBSr	0.96	0.32	–	12.27
1321−2725	NGC 5101	1.73	(R)SB(rs)0/a	0.0	R	0.92	0.56	2.66	12.26
1439+0521	NGC 5701	1.63	(R)SB(rs)0/a	0.0	R	0.84	0.25	1.49	13.25
1710+7218	NGC 6340	1.51	SA(s)0/a	0.0	R	0.79	–	2.80	12.90
2023−4359	IC 4946	1.39	SAB(rs)0/a:	−0.1	RCSr	0.72	0.21	–	12.17
0335−2456	NGC 1371	1.75	SAB(rs)a	1.0	R	0.85	0.44	1.21	12.70
0403−4321	NGC 1512	1.95	SB(r)a	1.0	R	0.75	0.13	0.62	13.39
0507−3730	NGC 1808	1.81	(R)SAB(s)a	1.0	R	0.74	0.23	2.36	12.60
1014+0328	NGC 3169	1.64	SA(s)ap	1.0	R	0.78	0.21	1.63	12.71
1023+1951	NGC 3227	1.73	SAB(s)ap	1.0	R	0.76	0.23	2.76	13.65
1222+2953	NGC 4314	1.62	SB(rs)a	1.0	R	0.81	0.26	–	12.13
1253+0210	NGC 4772	1.53	SA(s)a	1.0	R	0.83	0.26	2.41	11.36
1356+4714	NGC 5377	1.57	(R)SB(s)a	1.0	R	0.82	0.31	2.74	12.90
2144−7506	NGC 7098	1.61	(R)SAB(rs)a	1.0	R	0.79	0.35	–	13.32
2339−1217	NGC 7727	1.67	SAB(s)ap	1.0	R	0.84	0.35	4.87	12.32
0331−3337	NGC 1350	1.72	(R′)SB(r)ab	1.8	PBSr	0.77	0.26	2.69	12.57
0342−4713	NGC 1433	1.81	(R′)SB(r)ab	2.0	4	0.77	0.20	2.88	13.23
0910+0702	NGC 2775	1.63	SA(r)ab	2.0	R	0.83	0.32	4.50	11.92
0950+7216	NGC 2985	1.66	(R′)SA(rs)ab	2.0	R	0.68	–	1.55	–
0955+6904	NGC 3031	2.43	SA(s)ab	2.0	R	0.82	–	2.46	12.14
1031−3451	NGC 3281	1.52	SA(s)abp:	2.1	RBCSr	0.78	–	–	13.01
1046+1149	NGC 3368	1.88	SAB(rs)ab	2.0	R	0.79	0.25	2.89	12.40
1149+5605	NGC 3898	1.64	SA(s)ab	2.0	R	0.82	0.33	2.04	12.02
1250+2530	NGC 4725	2.03	SAB(r)abp	2.0	R	0.65	–	2.39	13.14
1250+4107	NGC 4736	2.05	(R)SA(r)ab	2.0	R	0.72	0.13	3.75	10.02
2203−3350	IC 5156	1.35	SB(s)abp:	1.6	PBSr	0.62	0.07	2.12	12.09
2207+3121	NGC 7217	1.59	(R)SA(r)ab	2.0	R	0.77	0.25	3.99	11.96

TABLE 15. (continued)

α (2000) δ	Name	$\log D_{25}$	Type	T	Source	$(B-V)_T^o$	$(U-B)_T^o$	H. I.	μ'_{eo}
0040−1352	NGC 210	1.70	SAB(s)b	3.0	R	0.63	0.01	1.08	13.86
0042+4116	NGC 224	3.28	SA(s)b	3.0	R	0.68	0.31	2.55	12.62
0121+0515	NGC 488	1.72	SA(r)b	3.0	R	0.79	0.28	3.28	12.73
0343−3551	NGC 1437	1.47	(R')SAB(rs)ab	2.5	RBCSr	0.68	0.13	–	12.77
0412−3252	NGC 1532	2.10	SB(s)bp sp	2.7	PBS	0.59	0.00	1.11	13.21
0936−2107	NGC 2935	1.56	(R')SAB(s)b	3.0	R	0.72	0.27	1.26	12.00
1021−3416	NGC 3223	1.61	SA(s)b	3.0	R	0.61	0.11	2.77	12.47
1043+1142	NGC 3351	1.87	SB(r)b	3.0	R	0.72	0.12	2.61	12.59
1231+1425	NGC 4501	1.84	SA(rs)b	3.0	R	0.60	0.15	3.39	12.48
1507+0132	NGC 5850	1.63	SB(r)b	3.0	R	0.72	0.13	2.74	14.17
1539+5919	NGC 5985	1.74	SAB(r)b	3.0	R	0.65	0.06	2.18	13.60
1716−6249	NGC 6300	1.65	SB(rs)b	3.0	4	0.59	−0.01	2.73	12.49
2218−3648	IC 5186	1.27	(R')SAB(rs)b:	3.2	PBSr	0.49	−0.09	–	12.19
0008−3351	NGC 10	1.38	SAB(rs)bc	3.6	PBSr	0.63	–	–	–
0319−1924	NGC 1300	1.79	SB(rs)bc	4.0	R	0.59	0.05	2.63	14.02
0339−3119	NGC 1406	1.58	SB(s)bc:	4.0	PSU	0.36	−0.17	1.70	12.40
0420−5456	NGC 1566	1.92	SAB(s)bc	4.0	R	0.56	−0.07	1.47	12.43
0727+8010	NGC 2336	1.85	SAB(r)bc	4.0	R	0.49	−0.03	1.98	14.22
0946−3026	NGC 3001	1.46	SAB(rs)bc	3.9	PSUr	0.59	−0.07	1.70	12.01
1153+5219	NGC 3953	1.84	SB(r)bc	4.0	R	0.66	0.12	3.16	13.34
1222+1549	NGC 4321	1.87	SAB(s)bc	4.0	R	0.65	−0.05	2.91	13.19
1316−1638	NGC 5054	1.71	SA(s)bc	4.0	R	0.64	0.09	2.58	13.06
1329+4711	NGC 5194	2.05	SA(s)bcp	4.0	R	0.53	–	2.81	12.45
1338−1752	NGC 5247	1.75	SA(s)bc	4.0	R	0.42	−0.20	2.55	13.56
1732+0703	NGC 6384	1.79	SAB(r)bc	4.0	R	0.55	0.11	1.76	13.75
2037+6606	NGC 6951	1.59	SAB(rs)bc	4.0	R	0.74	–	2.72	13.63
0136+1547	NGC 628	2.02	SA(s)c	5.0	R	0.51	–	0.99	13.54
0243+0122	NGC 1073	1.69	SB(rs)c	5.0	R	0.47	−0.12	1.36	14.28
0309−2034	NGC 1232	1.87	SAB(rs)c	5.0	R	0.59	−0.03	1.71	13.67
0317−3234	NGC 1288	1.36	SAB(rs)c	4.6	PBSr	0.63	0.01	2.64	13.46
0917−2221	NGC 2835	1.82	SB(rs)c	5.0	R	0.33	−0.23	1.58	13.22
1018−1758	NGC 3200	1.62	SAB(rs)c:	4.5	VSUE	0.55	0.07	1.19	13.05
1042+1344	NGC 3338	1.77	SA(s)c	5.0	R	0.51	−0.07	0.94	13.41
1054−2103	NGC 3464	1.41	SB(rs)c	5.0	PSUE	0.32	−0.13	1.66	–
1140+1128	NGC 3810	1.63	SA(rs)c	5.0	R	0.50	−0.13	2.17	12.16
1234+0811	NGC 4535	1.85	SAB(s)c	5.0	R	0.58	–	2.13	13.70
1337−2952	NGC 5236	2.11	SAB(s)c	5.0	R	0.61	−0.01	1.60	–
1819+7434	NGC 6643	1.58	SA(rs)c	5.0	R	0.50	−0.14	2.22	12.47
2125−4016	IC 5105A	1.33	SB(rs)c	5.1	RCSr	0.54	–	–	13.85
2304+1219	NGC 7479	1.61	SB(s)c	5.0	R	0.66	0.07	2.22	13.34
2347−3031	NGC 7755	1.58	SB(rs)c:	4.7	PSUr	0.62	0.01	1.39	12.90
0133+3039	NGC 598	2.85	SA(s)cd	6.0	R	0.47	−0.16	1.32	13.60
0221−0531	NGC 895	1.56	SA(s)cd	6.0	R	0.49	−0.08	1.26	13.69
0302−1853	NGC 1179	1.69	SAB(r)cd	6.0	R	0.56	−0.10	0.91	–
0417−6247	NGC 1559	1.54	SB(s)cd	6.0	R	0.31	−0.11	2.05	11.99
0736+6535	NGC 2403	2.34	SAB(s)cd	6.0	R	0.39	–	1.03	12.59
1243+1307	NGC 4654	1.69	SAB(rs)cd	6.0	R	0.54	−0.12	2.17	12.82
1318−2102	NGC 5068	1.86	SAB(rs)cd	6.0	R	0.58	–	1.69	12.77
1403+5421	NGC 5457	2.46	SAB(rs)cd	6.0	R	0.44	–	1.12	14.00
1609+0042	NGC 6070	1.55	SA(s)cd	6.0	R	0.52	−0.04	1.92	13.00
2034+6009	NGC 6946	2.06	SAB(rs)cd	6.0	R	0.40	–	2.28	12.30
2233−4056	NGC 7307	1.55	SB(s)cdp:	5.6	RBCS	0.22	−0.12	1.26	13.59
2343+2604	NGC 7741	1.64	SB(s)cd	6.0	R	0.46	−0.19	1.63	13.64
0054−3740	NGC 300	2.34	SA(s)d	7.0	R	0.58	0.11	0.58	–
0105−0612	A 0102−06	1.62	SAB(rs)d	7.0	R	0.68	0.07	0.76	–
0227+3334	NGC 925	2.02	SAB(s)d	7.0	R	0.50	–	1.04	14.32
0459−2601	NGC 1744	1.91	SB(s)d	7.0	R	0.48	−0.13	0.42	14.22
0920+6406	NGC 2805	1.80	SAB(rs)d	7.0	R	0.44	–	1.16	14.97
1118−3248	NGC 3621	2.09	SA(s)d	7.0	R	0.52	−0.15	0.88	12.06
1210+3952	NGC 4145	1.77	SAB(rs)d	7.0	R	0.50	−0.10	1.27	14.46
1233+0839	NGC 4519	1.50	SB(rs)d	7.0	R	0.51	0.02	1.00	–
1419+5643	NGC 5585	1.76	SAB(s)d	7.0	R	0.46	−0.22	0.95	14.29
1433+0427	NGC 5668	1.52	SA(s)d	7.0	R	0.65	–	1.25	13.16
1244−0540	A 1241−05	1.51	SAB(rs)dm	8.0	PEF	0.53	−0.09	0.80	14.58
0014−2311	NGC 45	1.93	SA(s)dm	8.0	R	0.69	−0.06	0.29	14.51
0101−0735	NGC 337A	1.77	SAB(s)dm	8.0	PE	0.44	−0.19	0.21	14.90
1159−1916	NGC 4027	1.50	SB(s)dm	8.0	R	0.52	−0.06	1.54	12.37
1207+0241	NGC 4116	1.58	SB(rs)dm	8.0	R	0.43	–	0.98	–
1217+4537	NGC 4242	1.70	SAB(s)dm	8.0	R	0.54	–	1.90	14.49
1232+0023	NGC 4517A	1.60	SB(rs)dm:	8.0	R	0.45	–	0.58	14.95
0112+0058	NGC 428	1.61	SAB(s)m	9.0	R	0.43	−0.20	0.90	13.42
0523−6945	LMC	3.81	SB(s)m	9.0	R	0.44	−0.05	2.14	–
0819+5000	NGC 2552	1.54	SA(s)m?	9.0	R	0.39	−0.19	1.32	14.63
1225+3332	NGC 4395	2.12	SA(s)m:	9.0	R	0.46	–	0.50	14.91
1241+4109	NGC 4618	1.62	SB(rs)m	9.0	R	0.44	−0.19	1.40	12.94
1329+5825	NGC 5204	1.70	SA(s)m	9.0	R	0.41	−0.33	0.76	13.26
1828−6658	IC 4710	1.56	SB(s)m	9.0	R	0.47	−0.17	1.72	–
0104+0208	IC 1613	2.21	IB(s)m	10.0	PUE	0.67	–	0.89	15.90
0259+2514	NGC 1156	1.52	IB(s)m	10.0	R	0.41	−0.31	1.25	12.28
1025+1709	NGC 3239	1.70	IB(s)mp	10.0	R	0.39	−0.36	1.02	12.52
1215+3619	NGC 4214	1.93	IAB(s)m	10.0	R	0.46	–	1.10	12.66
1228+4405	NGC 4449	1.79	IBm	10.0	R	0.41	−0.35	0.80	11.50
0555+0323	II Zw 40	–	cI	11.0	R	0.28	−0.32	–	–

restrictions. Among early-type galaxies ($T \leqslant 0$), the colors are redder for the high redshift sample than for the low redshift one. This is due to the selection of higher luminosity galaxies in the former sample and the well known color–absolute magnitude effect for early-type galaxies. The effect is most serious for $(U-B)_T^0$ as would be expected. In contrast to the early types, spirals in the range $2 \leqslant T \leqslant 6$ are bluer in the near sample than in the far sample. This is likely to be due to problems with the inclination corrections, in conjunction with a sample bias, for the following reasons. Firstly, Figs. 8(e) and 8(f) and 9(e) and 9(f) show that the inclination corrections adopted in RC3 are probably overcorrecting the colors for this type range. Secondly, the high redshift sample is biased against inclusion of highly inclined galaxies. Thus, it may not be surprising that the color-type correlations for the $V(3K) > 3000$ and $\log R_{25} \leqslant 0.20$ samples are very similar, as are the $V(3K) \leqslant 3000$ and $\log R_{25} > 0.20$ samples. The inclination corrections in RC3 were based on more restricted samples than used here and will be discussed in more detail in a separate paper.

In the hydrogen index plots (Fig. 10), we see that the low redshift sample emphasizes hydrogen-poor early types ($T \leqslant 4$) while the high redshift sample has an excess of hydrogen-poor late types ($T \geqslant 7$). The $\log R$ plots show some differences in the correlations for types in the range $2 \leqslant T \leqslant 6$, which may again be due in part to uncertainties in the inclination corrections. Note that these corrections are independent of the color corrections.

In the mean surface brightness plots (Fig. 11), the low redshift sample emphasizes higher surface brightness galaxies than the high redshift sample for all $T \leqslant 5$ (Sc), with the effect being especially pronounced for the types $T \leqslant 0$. This must reflect not only the absolute magnitude effect already noted in the colors, but also probably significant errors in the diameters A_e for the smaller galaxies in the catalogue. Figures 11(e) and 11(f) also show that the mean effective surface brightness is nearly constant over the range $-5 \leqslant T \leqslant 1$ for the $\log R_{25} \leqslant 0.20$ sample, and that the peak in mean surface brightness at $T = -2$ (S0°) in Fig. 7(e) is due mainly to highly inclined galaxies. Applying an internal absorption correction to the mean surface brightnesses would separate the low and high inclination samples even more than does the geometric correction in Eq. (12).

5.4 Representative Galaxies

With a large database of revised morphological types, it is possible to compile a list of galaxies which are representative of each revised Hubble stage. Up to a dozen typical galaxies at each morphological stage are listed in Table 15, which gives each galaxy's position, name, the logarithm of the isophotal diameter, the decoded revised full type, the mean numerical type index, the sources of the types used in the mean, the corrected colors, the hydrogen index, and the corrected effective surface brightness. The diameter is in units of 0.1. The list includes both northern and southern examples, and covers a range in each of the parameters discussed above. Note that a more complete list of types of the larger and brighter galaxies, updated to include RC3 data, will be presented as one of the appendices to the 1995 edition of *The Astronomical Almanac*.

6. SUMMARY

The monotonic relations of the colors, hydrogen index, and mean effective surface brightness with type reconfirm the order of the stages along the revised Hubble sequence. Even though galaxy classification is subjective, there is a high degree of correlation between experienced observers. This agreement allows us to combine the types from the various sources into reliable mean types. The color-type correlations illustrated in this paper can be explained in terms of the decreasing bulge-to-disk ratio (Simien & de Vaucouleurs 1986) and the increasing prominence of Population I stars from early to late types. The mean surface brightness-type correlation is also in part caused by the decreasing bulge-to-disk ratio with increasing type. The hydrogen index-type correlation can be partly explained by a systematic decrease in the total blue luminosity and also by an additional increase in the H I luminosity (and content) from early to late spiral types (de Vaucouleurs 1977; see Giovanelli & Haynes 1988 for a brief review of other aspects). Since some of the scatter in all of the correlations at a given type may be due to a spread in total luminosity, we should be able to improve the correlations by using as an independent variable the *luminosity index*, defined as a combination of type (T) and luminosity class (L) and which is a better indicator of absolute magnitude than T or L alone (de Vaucouleurs 1977, 1979). In a separate paper, we will make this combination for nearly 5000 spiral galaxies having mean luminosity classifications compiled by Odewahn & de Vaucouleurs (1992), and will reinvestigate the correlations discussed here.

This work was supported in part by NSF Grant Nos. AST-82-11735 and AST-85-13821 to the University of Texas (G. de Vaucouleurs, Principal Investigator) and by NSF EPSCoR Grant No. RII8996152 to the University of Alabama. We thank B. Skiff for sending his types in advance of publication, and a referee for helpful comments.

REFERENCES

Buta, R. 1978, Univ. of Texas Publ. Astron., No. 12
Buta, R. 1991, in Dynamics of Galaxies and Their Molecular Clouds Distribution, IAU Symposium No. 146, edited by F. Combes and F. Casoli (Kluwer, Dordrecht), p. 251
Buta, R., & Corwin, H. G. 1986, ApJS, 62, 255
Buta, R., & de Vaucouleurs, G. 1982, ApJS, 48, 219
Corwin, H. G. 1968, Publ. of the Dept. of Astron., Univ. of Texas at Austin, Series II, Vol. II, No. 12
Corwin, H. G. 1970, Publ. of the Dept. of Astron., Univ. of Texas at Austin, Series II, Vol. III, No. 5

Corwin, H. G., Buta, R., & de Vaucouleurs, G. 1994, AJ (submitted)
Corwin, H. G., de Vaucouleurs, A., & de Vaucouleurs, G. 1985, Southern Galaxy Catalogue (University of Texas Monographs in Astronomy No. 4, Austin)
de Vaucouleurs, G. 1956, Mem. Commonwealth Obs. 3, No. 13
de Vaucouleurs, G. 1959, Handbuch der Physik, 53, 275
de Vaucouleurs, G. 1963, ApJS, 8, 31
de Vaucouleurs, G. 1977, in The Evolution of Galaxies and Stellar Populations, edited by B. Tinsley and R. Larson (Yale University Observatory, New Haven), p. 43
de Vaucouleurs, G. 1979, ApJ, 227, 380
de Vaucouleurs, G., & Buta, R. 1980, AJ, 85, 637
de Vaucouleurs, G., & Corwin, H. G. 1986, ApJS, 308, 487
de Vaucouleurs, G., & de Vaucouleurs, A. 1964, Reference Catalogue of Bright Galaxies, University of Texas Monographs in Astronomy No. 1 (University of Texas Press, Austin) (RC1)
de Vaucouleurs, G., de Vaucouleurs, A., & Corwin, H. G. 1976, Second Reference Catalogue of Bright Galaxies, University of Texas Monographs in Astronomy, No. 2 (University of Texas Press, Austin) (RC2)
de Vaucouleurs, G., de Vaucouleurs, A., Corwin, H., Buta, R., Paturel, G., & Fouqué, P. 1991, Third Reference Catalogue of Bright Galaxies (Springer, New York) (RC3)
de Vaucouleurs, G., & Head, C. 1978, ApJS, 36, 439
Dressler, A. 1980, ApJS, 42, 565
Feigelson, E., & Babu, G. J. 1992, ApJ, 397, 55
Giovanelli, R., & Haynes, M. 1988, in Galactic and Extragalactic Radio Astronomy, edited by G. L. Verschuur and K. I. Kellermann (Springer, New York), p. 522
Hubble, E. 1926, ApJ, 64, 321
Lauberts, A. 1982, The ESO-Uppsala Survey of the ESO-B Atlas (European Southern Observatory, Munich)
Nilson P. 1973, Uppsala General Catalogue of Galaxies (Royal Soc. Sci. Uppsala, Uppsala) (UGC)
Nilson, P. 1974, Catalogue of Selected Non-UGC Galaxies, Uppsala Astron. Obs. Report No. 5 (UGCA)
Odewahn, S., & de Vaucouleurs, G. 1992, ApJS, 83, 65
Olson, D. W., & de Vaucouleurs, G. 1981, ApJ, 249, 68
Paturel, G., Fouqué, P., Buta, R., & Garcia, A. M. 1991, A&A, 243, 319
Sandage, A., & Tammann, G. A. 1987, A Revised Shapley–Ames Catalogue of Bright Galaxies (Carnegie Institution of Washington, Publ. No. 635) (RSA)
Schweizer, F., Ford, W. K., Jedrzejewski, R., & Giovanelli, R. 1987, ApJ, 320, 454
Simien, F., & de Vaucouleurs, G. 1986, ApJ, 302, 564

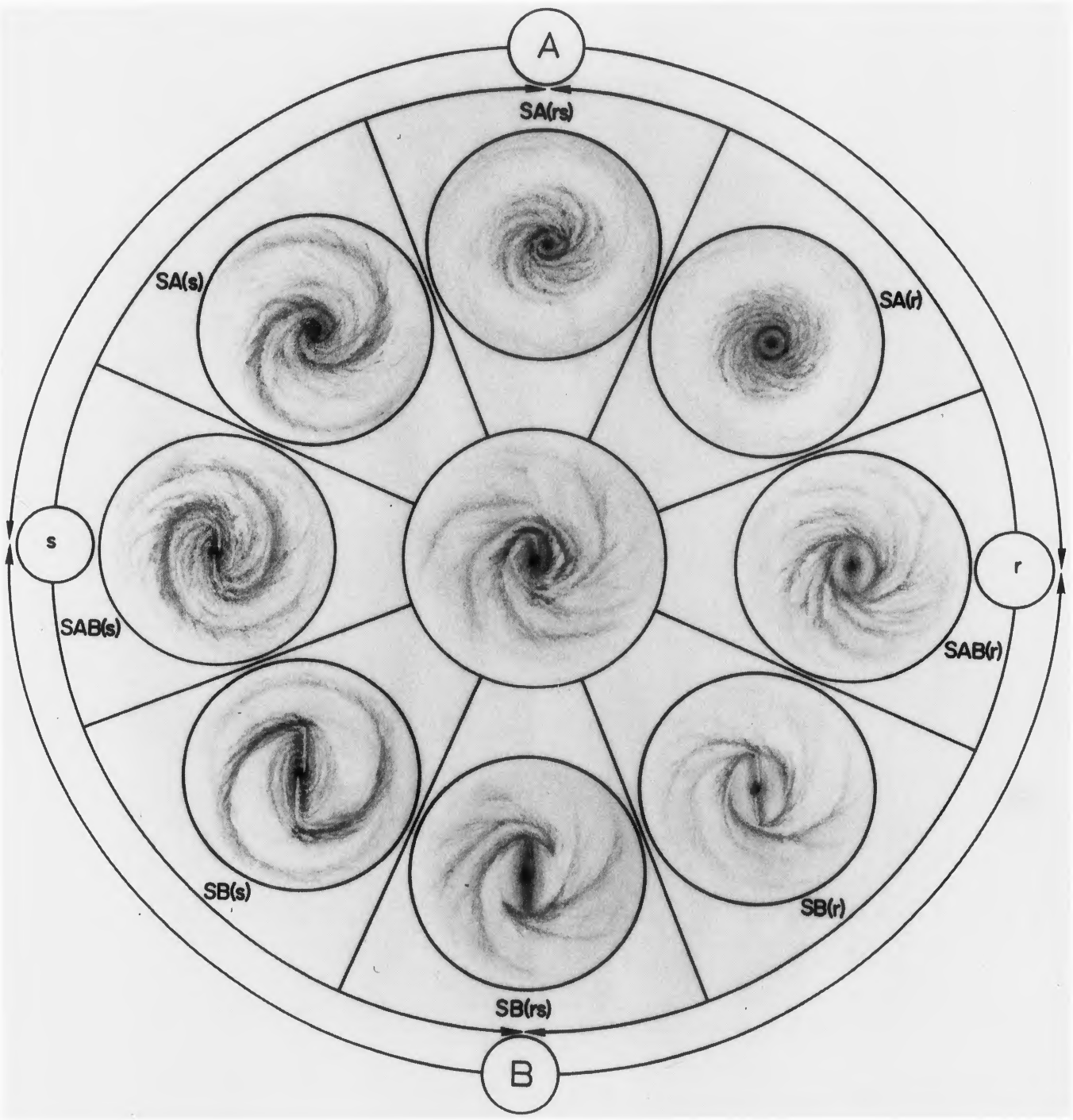

FIG. 1. Cross section of classification volume at stage Sb–Sbc showing typical structures of spirals of different families (A,AB,B) and varieties (r,rs,s).

Buta *et al.* (see page 119)